

IOWA STATE UNIVERSITY

Digital Repository

Graduate Theses and Dissertations

Iowa State University Capstones, Theses and
Dissertations

2018

Quantification of urban heat island impacts on the cooling energy consumption in residential and commercial buildings in the Continental United States

Saad Bin Tarik
Iowa State University

Follow this and additional works at: <https://lib.dr.iastate.edu/etd>

 Part of the [Geology Commons](#)

Recommended Citation

Tarik, Saad Bin, "Quantification of urban heat island impacts on the cooling energy consumption in residential and commercial buildings in the Continental United States" (2018). *Graduate Theses and Dissertations*. 16884.
<https://lib.dr.iastate.edu/etd/16884>

This Thesis is brought to you for free and open access by the Iowa State University Capstones, Theses and Dissertations at Iowa State University Digital Repository. It has been accepted for inclusion in Graduate Theses and Dissertations by an authorized administrator of Iowa State University Digital Repository. For more information, please contact digirep@iastate.edu.

**Quantification of urban heat island impacts on the cooling energy consumption in
residential and commercial buildings in the Continental United States**

by

Saad Bin Tarik

A thesis submitted to the graduate faculty

in partial fulfillment of the requirements for the degree of

MASTER OF SCIENCE

Major: Geology

Program of Study Committee:

Yuyu Zhou, Major Professor

William W. Simpkins

Zhengyuan Zhu

The student author, whose presentation of the scholarship herein was approved by the program of study committee, is solely responsible for the content of this thesis. The Graduate College will ensure this thesis is globally accessible and will not permit alterations after a degree is conferred.

Iowa State University

Ames, Iowa

2018

DEDICATION

To my family

TABLE OF CONTENTS

	Page
LIST OF FIGURES	v
LIST OF TABLES	vi
ACRONYMS	vii
ACKNOWLEDGMENTS	viii
ABSTRACT	ix
CHAPTER 1. INTRODUCTION	1
Background and Motivation	1
Research Questions and Objectives	3
Organization of the Thesis	4
CHAPTER 2. LITERATURE REVIEW ON UHI AND BUILDING ENERGY USE	5
UHI Formation and Quantification	5
Studies on the Quantification of Building Energy Consumption	9
Quantification of Building Energy Consumption and the Impact of UHI	10
CHAPTER 3. DATA AND METHODOLOGY	15
Study Area	15
Cooling Energy Consumption Data	16
Residential Cooling Energy Consumption Data	16
Commercial Cooling Energy Use Data	17
Temperature Data	17
Observed Temperature Data	18
Reanalysis Temperature Data	19
Grid-based Data	19
Impervious Surface Data	19
Elevation Data	20
Urban Extent Data	20
Population Data	20
Methodology	21
Calculation of Cooling Degree Days	21
Interpolation of Observed Cooling Degree Days	22
Quantile Regression of Cooling Energy Intensity	25
Floor Area Distribution and Total Energy Estimation	27
UHI Impacts on Cooling Energy Consumption	28

CHAPTER 4. RESULTS AND DISCUSSION	29
Comparison between Observed and NNR Degree Days	29
Interpolation of CDDs using Universal Kriging.....	31
Quantile Regression Estimation of Cooling Energy Consumption	35
Cooling Energy Consumption Intensity with Cooling Degree Days	35
Total Cooling Energy Consumption and the Impact of UHI	40
CHAPTER 5. SUMMARY AND CONCLUSION	46
Summary of the Results	46
Limitations and Future Directions	47
REFERENCES	49

LIST OF FIGURES

	Page
Figure 3.1: Census Divisions in the continental United States	16
Figure 4.1: Relation between GHCN-observed and NNR CDDs [$^{\circ}\text{F}$] in imperviousness levels of a) less than 20%, b) from 20% to 50%, c) from 50% to 70%, and d) greater than 70% of imperviousness.	30
Figure 4.2: CDDs in the urban areas of CONUS, a) estimated from UK, b) NNR CDDs, c) differences in CDDs from UK and NNR, and d) the relative histogram of the differences in CDDs	34
Figure 4.3: Validation statistics for predicted CDDs in $^{\circ}\text{F}$	35
Figure 4.4: Slope coefficients of cooling energy consumption intensity from quantile regression at different Census Divisions for a) residential and b) commercial buildings	37
Figure 4.5: Variations in slopes at different quantile levels for the a) residential and b) commercial buildings	39
Figure 4.6: Percent differences in median cooling energy consumption for (a) residential buildings and (b) commercial buildings	41
Figure 4.7: Cooling energy consumptions in (a) residential and (b) commercial buildings	43
Figure 4.8: Percent differences in aggregated cooling energy use between UHI and non-UHI cases for (a) residential and (b) commercial buildings.	44

LIST OF TABLES

	Page
Table 4.1: Mean slope coefficients for cooling energy consumption (thousand BTU/sq.ft./CDD) in all Census Divisions at different quantile levels	40
Table 4.2: Percent changes in median cooling energy use in all Census Divisions due to UHI (The ranges for 0.05-0.95 quantiles are given in the parentheses) holding other variables constant.	45

ACRONYMS

BTU	British Thermal Unit
CBECS	Commercial Building Energy Consumption Survey
CDD	Cooling Degree Days
CONUS	Continental United States
DEM	Digital Elevation Model
DMSP/OLS	Defense Meteorological Satellite Program/Operational Linescan System
EIA	Energy Information Administration
GHCN	Global Historical Climatology Network
NASA	National Aeronautics and Space Administration
NCAR	National Center for Atmospheric Research
NCDC	National Climatic Data Center
NCEP	National Center of Environmental Prediction
NLCD	National Land Cover Database
OLS	Ordinary Least Squares
OMR	Observed Minus Reanalysis
RECS	Residential Energy Consumption Survey
SRTM	Shuttle Radar Topography Mission
UHI	Urban Heat Island
UK	Universal Kriging

ACKNOWLEDGMENTS

First, I would like to express my sincere gratitude to my advisor Dr. Yuyu Zhou for his continuous support and providing constant guidance throughout my studies. His incredible supervision from the very beginning of my study has helped me to develop problem-solving skills which eventually led me to complete this study.

I would like to thank Dr. Xiaoma Li, Assistant Professor, Hunan Agricultural University, China for his constant supervision and instrumental guidance and sharing his vast experience that helped me to design and organize the study.

I would also like to thank Dr. William Simpkins and Dr. Zhengyuan Zhu for serving as committee members and also for their invaluable inputs during the program of study meeting which helped me to improve and broaden this thesis.

Special thanks to me fellow research group members (present and past) for sharing their knowledges and experiences which helped me to think differently and widen my knowledge. I am also thankful to my friends Esha Chatterjee, Dr. Sayan Choudhury, Dr. Yuan Xue, Dr. Lu Liu, Kanak Choudhury, Farhan Islam, Shoaib Mahmud, and Dr. Alfi Hasan for their support and encouragement.

I am always thankful to my family for their unwavering and persistent support throughout my life that helped me to grow as a better human being. Last but not least, I would like to express my special thanks to my beloved wife, Monoshe Rahman for being patient and providing strong support and continuous encouragement that helped me to complete this degree.

ABSTRACT

The Urban heat island (UHI) is a well-known phenomenon in an urban area where the urban core areas experience higher temperature than the surrounding rural areas. It has numerous implications among which building energy consumption is a prominent one. This study investigates the UHI effects on the building energy consumption for cooling in the urban areas of the Continental United States (CONUS). To account for UHI effects, long-term differences in mean annual cooling (CDDs) between observations from Global Historical Climatology Network (GHCN) and the urbanization-insensitive National Center for Environmental Protection-National Center for Atmospheric Research 50-year Reanalysis (NNR) from the years 2008 to 2017 are used. Cooling energy consumption data from surveyed buildings by the Energy Information Administration were used to identify the relationship between cooling energy consumption intensity and CDDs and other covariates related to building characteristics. Using universal kriging and observed minus reanalysis (OMR) method, it has been found that there will be up to 2,509 additional cooling degree days annually in the urban areas due to the UHI effect. Quantile regression results using CDDs and other covariate show that show that a unit increase in CDD will cause an average increase in median cooling energy use intensity by 2.1 BTU/sq.ft. (residential) and 2.5 BTU/sq.ft. (commercial). The mean increase in cooling energy consumption in selected building type, building construction year, and the number of occupants is 28.1% for commercial buildings and 22.9% for residential buildings in all Census Divisions.

CHAPTER 1. INTRODUCTION

Urban heat island (UHI) is a major phenomenon that is observed in urban areas around the world. It is observed when urban areas have higher temperature compared to the surrounding rural/non-urban areas (Oke 1973; Landsberg 1981; Peng et al. 2012; Bokaie et al. 2016; Xiaoxiao Li et al. 2016; Vahmani and Ban-Weiss 2016). The replacement of natural surfaces by building materials in urban areas causes a decrease in evaporative cooling and resulting in elevated temperature in the urban area. UHI has numerous implications ranging from environmental degradation, human health, and energy use in buildings. With the increasing population and urban size and resulting increase in UHI phenomenon globally, it is essential to understand its processes to assess impacts on human life and environment with higher accuracy as well as identify mitigation measures to reduce its harmful effects.

Background and Motivation

Many parts of the world are experiencing rapid urban growth recently, especially the developing countries (Peng et al. 2012). The United Nations estimated that about 60 percent of the population of the world would live in cities by 2030 which will lead to the expansion of impervious surface area; i.e., urban area (Chun and Guldmann 2014). Increasing population in the urban area also leads to increase vehicular traffic, human metabolism activities, and emissions from daily appliances, which are likely to intensify UHI phenomenon in urban areas (Menberg et al. 2013). Building energy consumption is sensitive to ambient temperature and among many impacts of UHI phenomenon, elevated temperature in urban areas cause increases the energy use in buildings for cooling purposes which leads to an increase in electricity production, fuel usage, anthropogenic heat release, and relevant

air pollution (Mat Santamouris 2007; M. Kolokotroni et al. 2012; Lundgren and Kjellstrom 2013; Arifwidodo and Chandrasiri 2015).

The building sector is a significant consumer of energy in the United States. Energy consumption in a building is dependent upon many factors. Outdoor temperature plays a significant role in energy requirements in buildings (Ewing and Rong 2008; Kaza 2010; Min, Hausfather, and Lin 2010). In addition to outdoor temperature, building characteristics such as age, size, types, and materials used influence energy consumption (Ewing and Rong 2008; Kaza 2010; Min, Hausfather, and Lin 2010). Among the socioeconomic factors, the number of occupants, household composition, income level, and race are also substantial (Ewing and Rong 2008). In 2017 in the United States, the building sector consumed nearly 39 percent of the total energy, followed by the industrial sector (32 percent) and transportation sector (29 percent) (EIA 2018).

Most current studies of UHI are limited to a smaller spatial scale. For example, they usually focus on UHI effects on energy use in a particular city using observational networks in urban areas and surrounding rural (i.e., non-urban) areas taken from weather station data or mobile measurement data (Oke and Maxwell 1975; Streutker 2003; Kim and Baik 2005; Jones, Lister, and Li 2008; Charabi and Bakhit 2011; Mat Santamouris et al. 2017). Several studies have assessed the influences of UHI on the energy use in a particular type of model building (e.g., typical residential, office, or commercial building) using building energy simulation software (Maria Kolokotroni, Zhang, and Watkins 2007; M. Kolokotroni et al. 2012; Magli et al. 2015; Vallati et al. 2015; Skelhorn, Levermore, and Lindley 2016). The sparse observational network in the highly-developed urban core or center areas limits our understanding of urban temperature and the corresponding UHI effect. The scarcity of the

observations of temperature in the urban area often leads to only rely on one urban and one rural station for UHI quantification (Landsberg 1981; Ackerman 1985; Fortuniak, Kłysik, and Wibig 2006). Such results often raise concerns regarding the representation of urban and rural temperature and the UHI intensity (Schatz and Kucharik 2016). Moreover, it is crucial to understand better the cooling energy use resulting from UHI in the US that is not limited to a particular city or hypothetical building. This research serves as a preliminary attempt to understand the UHI impacts and corresponding energy consumption for cooling in the urban areas of the Continental United States (CONUS).

Research Questions and Objectives

To address the limitations of the current status of the impacts of UHI on cooling energy consumption, the following research questions are explored by this thesis:

1. What are the effects of urban heat island on the cooling degree days (CDDs)?
2. How does the cooling energy consumption relate to the CDDs in the buildings of the US?
3. How will the energy consumption for cooling change in buildings in response to the increased CDDs from UHI?

To answer the above-mentioned research questions, firstly the cooling degree days will be estimated in the urban areas of the United States from temperature data to quantify UHI effect. Then, using residential and commercial cooling energy consumption data, the relation between cooling energy consumption and cooling degree days will be estimated. Finally, this relation will be used to quantify the increase in cooling energy cooling consumption due to the degree days resulted from UHI effects.

Organization of the Thesis

This thesis is organized in five chapters. The contents of each chapter is provided below:

1. Chapter 1: This is the introductory chapter for the thesis. This chapter includes background information, motivations, research questions, and objectives.
2. Chapter 2: This chapter includes a literature review on the UHI formation, quantification, overview of the energy use in the US, and the impacts of UHI on energy consumption.
3. Chapter 3: The data used in the study is described in this chapter along with the overview of the study area. The methodologies followed in the study are also described here.
4. Chapter 4: This chapter includes the results and discussions from UHI quantification and its impacts on cooling energy consumption.
5. Chapter 5: The final chapter summarizes the results from the study. It also includes the limitations and future directions.

CHAPTER 2. LITERATURE REVIEW ON UHI AND BUILDING ENERGY USE

UHI Formation and Quantification

UHI generation is a complex process. UHI is triggered by the replacement of the natural surface with building and road materials (e.g., asphalt and concrete) during the urbanization process (Vardoulakis et al. 2013; Heini et al. 2015). As a result, the reduction of evapotranspiration causes a reduction of latent heat flux from the surface (Susca, Gaffin, and Dell’Osso 2011). In contrast, sensible heat flux in the surface increases (Oke and Maxwell 1975; Azevedo, Chapman, and Muller 2016; Vahmani and Ban-Weiss 2016). Building materials and road surfaces absorb more heat than the natural surface during the daytime. When they re-emit the longwave radiation back to the atmosphere during nighttime, the UHI effects become more prominent (Goward 1981; Kim and Baik 2005; Arifwidodo and Chandrasiri 2015). UHI is controlled by different anthropogenic and natural and weather-related factors (Rizwan, Dennis, and Liu 2008). Processes that contribute to the UHI effect include urban geometry and layout, local weather pattern, anthropogenic heat emissions from metabolic activities in human, appliances, and transportation sector, and urban sprawl (Oke 1987; Stone, Hess, and Frumkin 2010; Schwarz and Manceur 2014; Azevedo, Chapman, and Muller 2016). UHI is mainly measured as an intensity, which is the difference between measured temperature between urban and rural areas where the temperature of the rural areas is taken as the “reference” temperature (Charabi and Bakhit 2011; Vardoulakis et al. 2013; Imhoff et al. 2010; Watkins et al. 2002). Temperatures are measured using ground-based stations or mobile stations mounted in vehicles. The mobile stations mounted on vehicles measure the temperature continuously by traveling from urban to rural areas.

There are two types of UHI that are usually measured-surface and air UHI. These are obtained from surface and air temperature differences from urban and surrounding rural areas, respectively. The most traditional method of determining the UHI is the calculation of the differences in the temperature between urban and rural areas. This method is generally termed as the “urban minus rural” method for detecting UHI intensity. Increased temperature in urban areas increases the CDDs. For example, Landsberg (1981) found an increase of CDDs between 8% and 93% across several major cities in the United States which accounts for additional 112 to 574 CDDs [$^{\circ}\text{F}$] annually from 1941 to 1970 using a pair of urban and rural observational network. However, Schatz and Kucharik (2016) argued that using only a pair of stations for quantifying UHI intensity is a concern because of the representativeness of urban and rural temperatures and replicability. Using an observational network of 26 ground-based stations in the Twin Cities Metropolitan Area, Minnesota, United States, Todhunter (1996) found about 617 additional CDDs [$^{\circ}\text{F}$] annually in the central urban area in the year 1989. Several studies explored the impact of population, urban size, and the impervious surface on the UHI. Tran et al. (2006) studied the surface UHI in 18 megacities in Asia using remotely-sensed land surface temperature (LST). They found that there are positive correlation between UHI and population and city size. Using Moderate Resolution Imaging Spectroradiometer (MODIS) data, Clinton and Gong (2013) identified development intensity, vegetation, and urban size are essential factors for UHI prediction. Using MODIS LST from nearly 5000 urban areas in the CONUS, Li et al. (2017) found that urban area size explains 87% of the total variations in surface UHI. MODIS LST was also used by Huang et al. (2017) who found the canopy layer UHI ranges from 1.0 to 2.2 $^{\circ}\text{C}$ for Terra and Aqua overpasses, respectively, for the period 2000-2013 in Shanghai, China. Their study also

found approximately 1.0°C annual nighttime UHI. Impervious surface is an essential factor in determining the LST. A study by Imhoff et al. (2010) found that the impervious area significantly contributes to the increase in LST. They also found that the impervious area explains nearly 70% of the total variations in LST. Using three-dimensional, numerical modeling of UHI, Atkinson (2003) found that anthropogenic heat discharge makes nighttime UHI intensity prominent while reduced evaporation determines daytime UHI intensity.

Geospatial interpolation methods from ground-based stations are also used in several studies to identify UHI effects which bridge the gap of scarce temperature observational network in urban locations. Smoliak et al. (2015) interpolated hourly temperature data from ground-based station network to 1 km × 1 km grid using kriging and co-kriging methods in the Twin Cities Metropolitan Area in Minnesota, United States. They used the impervious surface as an explanatory variable for the kriging and co-kriging interpolation. In Oklahoma City, the strongest UHI intensity was found in the highly-developed urban center with high surface roughness due to the buildings (Hu et al. 2016). This study also used the kriging interpolation method. Kriging was found to perform better than linear regression to estimate the daily temperature in the Detroit metropolitan area using surface imperviousness and distance-to-water as explanatory variables (K. Zhang et al. 2011). Schatz and Kucharik (2014) used regression-kriging in their study to interpolate monthly average temperatures using percent imperviousness of the land surface, lake effect, and topographic relief (the difference between the elevation and the average elevation within an area with 0.8-km of radius obtained from elevation datasets at 3 meters of resolution) in Madison, Wisconsin, United States. In their study, the temperature increase was approximately 1.5°C with an increase of impervious area from 0% to 30%. Another study by Schatz and Kucharik (2016)

found that there are up to 313 additional CDDs [$^{\circ}\text{F}$] using an observational network of 150 stations and regression-kriging from 2012-2015.

In Fuzhou and Xiamen cities in China, the increase in LST was found to increase at an exponential rate (Xu 2010). Another study by Xu et al. (2013) compared the contribution from the impervious area versus the contributions from vegetation and water bodies. This study found that the contribution from the impervious area in LST is almost six times higher than the contribution from the vegetation and water bodies. This study also found a very high correlation between impervious surface and LST which ranges from 0.853 to 0.930.

Kalnay and Cai (2003) developed another method to understand the influence of urbanization and land-use changes on temperature. This method is commonly known as the “observed minus reanalysis” (OMR) method (Kalnay and Cai 2003). They used the temperature dataset from the National Centers for Environmental Prediction (NCEP) National Center for Atmospheric Research (NCAR) 50-year Reanalysis (NNR) and observed temperature data from the ground-based stations to estimate the impact of urbanization and the changes in other land-uses on the temperature trends. The difference between the observed and the reanalysis temperature products (i.e., OMR) can be attributed to urbanization and changes in land-uses because the NNR temperature data is insensitive to surface characteristics including urbanization (Kalnay and Cai 2003; Kalnay et al. 2006; Ewing and Rong 2008). NNR surface temperatures are estimated from the atmospheric values where it is influenced by atmospheric vertical soundings (rawinsondes and satellites) which makes it insensitive to urbanization and land use. However, NNR shows the impacts of climate change as observed by ground-based stations (Kalnay and Cai 2003). Further details on NNR datasets are provided in the following chapter.

The primary advantage of the NNR dataset is that it does not require to classify the ground-based stations as “urban” or “rural” to quantify the impacts of urbanization. Classifications of the ground-based stations are done usually using population data (Easterling et al. 1997) and night lights data (Kevin P. Gallo, Easterling, and Peterson 1996; K.P. Gallo et al. 1999; Hansen, Ruedy, and Sato 2001). Using ground-based observations and NNR data Kalnay and Cai (2003) found the average trends of $+0.088^{\circ}\text{C}/\text{decade}$ and $+0.061^{\circ}\text{C}/\text{decade}$, respectively. The differences between these two trends can be attributed to the impacts of urbanization and other land-use changes. Many other studies adopted the OMR method. Zhou et al. (2004) estimated the impact of urbanization in the southeastern part of China using OMR method and found a warming trend of $0.05^{\circ}\text{C}/\text{decade}$. They attributed the observed trends to urbanization. Yang et al. (2009) found a warming trend of 0.14°C per decade from 1960 to 1999 using OMR method. Another study by Yang et al. (2011) found the OMR trends in the metropolis and large cities in China are 0.398°C and 0.26°C per decade. The daily mean surface temperature warming trend was found to be 0.12°C per decade using OMR method in China from 1960 to 1999 (Jingyong et al. 2005). The same study also found the trends of $0.20^{\circ}\text{C}/\text{decade}$ and $0.03^{\circ}/\text{decade}$ in maximum and minimum temperatures, respectively. Rong (2006) used the OMR method to calculate the increase in cooling degree days in the continental United States. The study calculated the difference in cooling degree days from ground-based stations and NNR data and found that there are 17% to 233% more CDDs in the observation data compared to the NNR data in different Census Divisions of the United States (Rong 2006).

Studies on the Quantification of Building Energy Consumption

Building energy consumption is sensitive to ambient temperature, and hence UHI has a considerable impact on it. Building energy consumption is also influenced by building type,

age, occupancy, functions, and socioeconomic variables (Rong 2006; Ewing and Rong 2008; Min, Hausfather, and Lin 2010; Azevedo, Chapman, and Muller 2016). The United States Energy Information Administration (EIA) estimated that the total electricity consumption in buildings is about 2.73 trillion kWh (EIA 2018). Energy consumption in buildings is almost 40 percent of the total energy in the US and almost 74 percent of the total electricity (EIA 2018).

Quantification of Building Energy Consumption and the Impact of UHI

The calculation of building energy consumption can be divided into two broad categories: top-down and bottom-up methods. These two methods can be subdivided into simulation- and physics-based models, statistical approaches, machine learning methods, and other methods (Li et al. 2017; H. Zhao and Magoulès 2012; Ko 2013; Swan and Ugursal 2009). According to Li et al. (2017), top-down methods consider a set of buildings and energy consumption is estimated at building levels without taking into account the differences among buildings. The study also described the bottom-up approaches where each building and their energy end-uses are modeled that could be further aggregated to the city, state, or country level. Hirano and Fujita (2012) developed estimation equations for specific energy consumption using survey data and calculated UHI impact on building specific energy consumption. They used two scenarios to compute the UHI impacts: a “present case” that represents the present scenario in the urban area with the built-up area and UHI phenomena and a “non-UHI case” where the built-up area is replaced by forest and wasteland. The temperature was simulated for both “present case” and the “non-UHI case” so that the UHI impact on temperature can be estimated. Their study found that space cooling energy consumption in both residential and commercial buildings is increased by 27.5 percent annually due to the UHI effect (Hirano and Fujita 2012). The combined energy

consumption increased by 1 percent in the commercial sector but decreased by 8 percent in the residential sector. The study also found that the total energy consumption decreased by 3.7 percent. Building energy simulation software are widely used in building energy consumption calculations. Cui et al. (2017) investigated the spatiotemporal characteristics of UHI in Beijing and its impact on building energy consumption. The study used temperature data from urban and rural stations and found significant UHI in Beijing with a maximum urban-rural difference of 8°C in winter. They also concluded that due to UHI, the cooling load in the urban areas are 11% higher than that of rural areas. Liao et al. (2017) found the relation between surface urban heat island and energy consumption during daytime and nighttime separately in 32 major cities mainland China. They calculated surface heat island intensity using MODIS LST and used the correlation between energy use and nighttime light data to compute energy use intensity. Their study found positive correlation at the nighttime which was significant but no correlation during the daytime. Howard et al. (2012) studied the spatial distribution of energy consumption in New York City. The study assumed that only building function determines the energy use rather than building type and age. They used regression analysis for the building energy consumption estimation using building floor area as a predictor. The spatial distribution of space cooling shows that higher values are concentrated around the central business district in Manhattan which represents the impact of UHI. Building energy simulation software are widely used to estimate building energy consumption. Heiple and Sailor (2008) used eQuest (DOE2 2008) for the downtown Houston, Texas. They found that the downtown area energy consumption is higher than that in the surrounding area due to the UHI phenomena (Heiple and Sailor 2008). Zhou et al. (2012) also used eQuest for building energy modeling and found that with a mean increase in

anthropogenic heat release of 32 W/m^2 , the residential and commercial energy consumption increase by 5.5 W/m^2 . Skelhorn et al. (2016) simulated the building energy consumption and compared it with a “base” scenario of a suburban setting. They found that UHI increases the building energy requirements ranging from 9.4 percent to 12.2 percent in a model office building (Skelhorn, Levermore, and Lindley 2016). Bagiorgas and Mihalakakou (2016) used TRNSYS (Solar Energy Laboratory 1997), a building energy modeling software for the Greater Athens Area in Greece. Their study found that cooling load is almost four times higher for a school building for the central location compared to the rural location (Bagiorgas and Mihalakakou 2016). Their study also explored the artificial neural network method to identify the contributions from urban and climatological parameters and found that the urban heat island is the major variable that controls the energy consumption in a typical school building. Also in Athens, Greece, a study by Santamouris et al. (2001) found that the UHI intensity is about 10°C which raised the cooling energy use in the urban areas two times and the peak electricity load to be tripled. According to a study by Sailor (2001), one extra cooling degree day could increase the electricity consumption in commercial buildings by 0.200 to 0.572 kWh per capita and in residential buildings by 0.283 to 1.177 kWh per capita. Using TRNSYS, Magli et al. (2015) found that the summer cooling energy uses in buildings are 10% higher in urban areas compared to a suburban area. Berger et al. (2014) found the impact of UHI in Vienna, Austria as the difference of 5 kWh/m^2 between the urban and semi-urban locations. Fung et al. (2006) investigated the influence of temperature increase in residential, commercial, and industrial sectors. Their study found that annual electricity consumption increases by 9.2%, 3%, and 2.4% in these three sectors, respectively, with a 1°C increase in monthly temperature (Fung et al. 2006). The climate sensitivity of building

energy consumption was studied by Brown et al. (2015), and it was found that an increase of 10 CDDs would increase the energy consumption by 11 to 16 percent in residential and commercial buildings. In the US cities with a population greater than 100,000, Akbari et al. (1992) found the increase in electricity load is almost 2% for every 1°F increase in the outside temperature due to UHI. Santamouris et al. (2001) reported that since 1940, the city of Los Angeles had experienced an increase of 1.5 GW electricity demand due to UHI. In Singapore, the increase in urban temperature of 1°C will cause an increase of 33 GWh of electricity demand annually in the next 50 years (Tso 1994). Kolokotroni et al. (2012) modeled the energy consumption in a modeled office building due to the UHI effect. The study found that energy consumption is five percent higher compared to surrounding rural locations. Ojima (1991) investigated the heat island phenomena in Tokyo, Japan. He found that from 1965 to 1975, the cooling load in the buildings increased by 10% to 20%. Kikegawa et al. (2003) also explored the UHI effect in Tokyo. They developed a numerical simulation model that integrates urban canopy meteorological model and building energy model. The study found that the peak electricity demand increases by 3% per 1°C increase in temperature which is equivalent to 1.5 GWh. Li et al. (2014) considered humidity and cumulative effect in addition to urban heat island effect and found an increase in summer electricity consumption by 11.28% in Beijing in the year 2005. In Bangkok, Thailand, monthly consumption data were used, and it was found that cooling degree days explain almost 88 percent variations in energy use per square meter (Arifwidodo and Chandrasiri 2015). Cooling degree days has been found to be the largest contributing factor compared to other variables for energy consumption (Lam 1998). Using regression with cooling degree days as an explanatory variable, Radhi and Sharples (2013) estimated air-conditioning use

and found that CDDs increase by 17 to 19 percent in urban areas and increased use of air-conditioning by 10 percent. Kaza (2010) used quantile regression for residential energy use patterns in the United States. The study found that in addition to the climate-related variables, household size is a key variable in cooling and other energy consumptions. Rong (2006) used multiple regression between energy use in households and household and climate-related variables. The study found that ten additional cooling degree days will lead to an increase in primary energy consumption for space cooling by 90,000 thousand BTU (Rong 2006).

CHAPTER 3. DATA AND METHODOLOGY

The overarching goal of this study is to quantify the impact of urban heat island on building electricity consumption for cooling purposes. There are two types of buildings considered in the study, commercial and residential buildings. Temperature data are used to quantify the UHI effect as well as to understand its impacts on building energy use. Other data used in the study are impervious surface data, population data, and urban nightlight data. The following subsections include the details of these datasets.

Study Area

This study encompasses the entire continental United States (CONUS). CONUS consists of 48 states (states excluding Alaska and Hawaii) and the District of Columbia. Cooling energy consumption due to UHI is estimated based on quantile regression models in the Census Divisions which are defined by the United States Census Bureau. There are 9 Census Divisions in the United States where each of them consists of multiple states. Survey data from residential and commercial buildings report the location of the buildings as their Census Divisions shown in Figure 3.1. The urban area extents obtained from nightlight data (discussed in the Data section) is also shown in the figure. These urban areas have a mean elevation lower than 500 meters, which is used in OMR-based studies since the correlation between observed and reanalysis temperature is weak in the regions above 500 meters of elevation (Kalnay and Cai 2003).

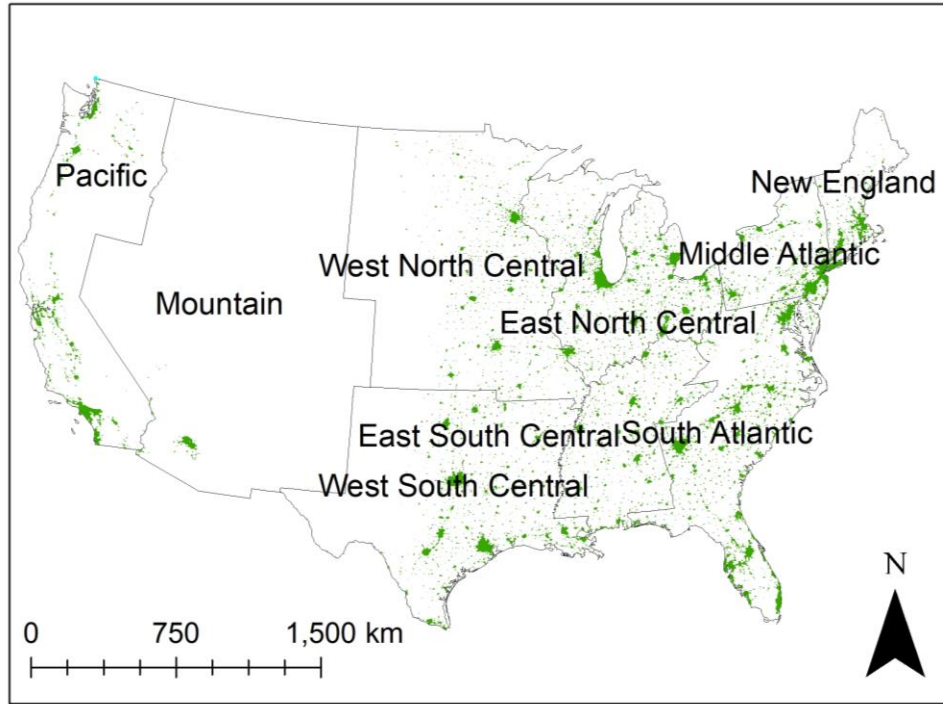


Figure 3.1: Census Divisions in the continental United States

Cooling Energy Consumption Data

Residential Cooling Energy Consumption Data

Residential cooling energy consumption data is obtained from the Energy Information Administration's (EIA) Residential Energy Consumption Survey (RECS) dataset. The first survey was held in 1978, and since then it has been conducted every few years. The latest survey was conducted in 2015 which is used in this study. RECS surveyed 5,687 households in total across all 50 states and the District of Columbia in the United States. The survey dataset contains different types of variables to characterize the household type, characteristics, age, and size and socioeconomic variables such as occupants, race, and income level. Data pertaining to the energy use such as fuel type, fuel usage, and price are also included in the dataset. It also provides a weight for the surveyed household. This weight is representative of the probability of the house is being selected. In other words, the

weight represents the surveyed household and other households with similar characteristics that were not surveyed. Therefore, the sum of the weights from each household represents the total number of households in the entire United States. This weight is helpful for calculating the national-level consumption, such as total and average consumption from the surveyed household data.

Commercial Cooling Energy Use Data

The cooling energy usage data in commercial buildings are collected from the Commercial Building Energy Consumption Survey (CBECS). This survey was also administered by the EIA which recognizes commercial buildings as those buildings where at least half of the available floor space is not used as residential, industrial, or agricultural purposes. Therefore, buildings such as schools, hospitals, buildings for religious purposes are also considered as commercial buildings in addition to the buildings that are used as shopping malls, offices, and other commercial purposes. This dataset also includes the type of buildings, age, building type and functions, floor space, fuel usage, and other variables. The observed cooling degree days (CDDs) based on 65°F at the building location are also available in the CBECS data. In 2012, CBECS surveyed 6,720 commercial buildings in the United States. Its Census Division provides the geographic location of the surveyed buildings. The dataset also uses sampling weights which represent the number of commercial buildings that have similar characteristics as the surveyed building.

Temperature Data

Temperature data from two sources were used to quantify the UHI impacts. The cooling degree days (CDDs) were calculated from daily mean temperature data that reflect the cooling energy requirement in a building. Another set of CDD data were used from the RECS and CBECS data from the building-level survey data. These CDD data were used to

quantify the relationship between cooling energy consumption and CDD. Temperature data are collected for a 10-year time period between 2008 and 2017. The time period covers the data collection periods for both RECS and CBECS data. Using multiyear data and taking their mean allows removal of any unusual or extreme events for a particular year and provides a more general picture of the temperature dataset (Rong 2006). In the following subsections the details for the observed and the reanalysis dataset are provided.

Observed Temperature Data

The observed temperature data were obtained from the Global Historical Climatology Network (GHCN) dataset from the National Climatic Data Center (NCDC) (Lawrimore et al. 2011; Menne et al. 2012; Vose et al. 1992). The GHCN data are mainly observations from ground-based stations. These stations provide maximum and minimum temperatures, precipitation, pressure, and other observations. Maximum and minimum temperature data were used from the GHCN stations to calculate the CDDs. There are some quality control applied to the raw GHCN dataset. Many GHCN stations suffer from missing either maximum or minimum or both temperatures for certain days of the year. If the missing data for a particular station is more than 30% in a particular year, then that station was not included in the study. To estimate the missing CDDs, long-term daily mean CDDs are calculated from the mean temperature (one CDD = Mean Temperature of the day – 18°C; more details on calculating degree days are provided in the Methodology section). The sum of the long-term mean daily cooling degree days was calculated excluding the days with missing temperature and hence the cooling degree days. The sum of available CDDs for a particular year was calculated, then the ratio was calculated between these two numbers. The long-term mean CDDs from the day of missing temperature was divided by the ratio to obtain the missing CDDs for the particular day in that particular year.

Reanalysis Temperature Data

Another set of temperature data was used in the study is the temperature data from National Center for Environmental Prediction (NCEP) National Center for Atmospheric Research (NCAR) 50-year Reanalysis (NNR) data (E. Kalnay et al. 1996; Eugenia Kalnay and Cai 2003). As the name implies, this is a reanalysis product available in 2.5×2.5 degree resolution, which re-gridded to 1-km resolution. This dataset is not sensitive to surface characteristics such as urbanization and land-use changes. This dataset did not use surface observations of temperature, moisture, and winds; instead, it used data from atmospheric and satellite soundings which is why it does not correspond to the surface characteristics (Kalnay and Cai 2003; Kalnay et al. 2006; Ewing and Rong 2008). Surface temperatures are estimated from these data. Similar to GHCN data, NNR data were collected from the period 2008-2017, and the long-term annual mean was calculated.

Grid-based Data

Impervious Surface Data

The National Land Cover Dataset (NLCD 2011) (Homer et al. 2015) was used in the study to identify the level of imperviousness, i.e., urbanization. In urban areas, impervious surfaces are prevalent since there are buildings, roads, and parking lots. In a densely-built urban area, the surface imperviousness level is higher compared to a low-density urban area. NLCD data provides the national-level land cover information at 30-meter resolution. The percent imperviousness dataset provides the urbanization level at a grid-level where the percentage depicts the portion of a grid-cell covered by the impervious surface. Therefore, a higher percentage indicates a higher density urban area. The impervious surface area is resampled to 1 km grid-cell and the average value of imperviousness from surrounding $1 \text{ km} \times 1 \text{ km}$ area of a particular grid was used as the percent imperviousness of that grid.

Elevation Data

Elevation data were obtained from the National Aeronautics and Space Administration's (NASA) Shuttle Radar Topography Mission (SRTM). This dataset provides a very high-resolution digital elevation model (DEM) of the surface. The space shuttle Endeavour completed an 11-day mission in the space to collect the elevation data at a resolution of 30 m using C-band (6 cm) Spaceborne Imaging Radar and X-band (3-cm) Synthetic Aperture Radar. Similar to the NLCD data, this dataset was also resampled to 1 km grids. The average value of the 1 km \times 1 km area surrounding a grid-cell was used as the elevation of the grid cell.

Urban Extent Data

Urban maps derived from the nightlight data were used in the study (Zhou et al. 2014; Zhou et al. 2015). These were derived using a cluster-based method from the stable nightlight (NTL) from the Defense Meteorological Satellite Program/Operational Linescan System (DMSP/OLS). The derived urban map product achieved a very high accuracy of 91% in the US; urban areas cover about 2% land area in total in the US with a range from 0.5% to 10% at state levels (Zhou et al. 2014).

Population Data

The US Census Grid (Summary File 3, 2000) provides a grid-level population data including other demographic and socioeconomic data (Seirup and Yetman 2006). These data are produced by the Columbia University Center for International Earth Science Information Network (CIESIN) (Columbia University 2017) at 30 arc-second grid. Similar to the NLCD and elevation data, this data was also resampled to the 1-km grid cell.

Methodology

Calculation of Cooling Degree Days

Cooling degree days are used to quantify the cooling energy requirements in buildings which are calculated from daily mean temperature data. Hence, cooling degree days reflect the requirement for cooling energy in buildings. Degree days are calculated as the deviations from a base temperature. The most frequently used base temperature for degree days is 18°C (65°F) (Landsberg 1981; Todhunter 1996; EPA 2014; EIA 2017); however, some studies set the base temperature empirically (Isaac and van Vuuren 2009). If the mean daily temperature is higher than the base temperature, it is assumed that the building requires cooling and the differences between the mean temperature and the base temperature are calculated as cooling degree days for the day. The daily CDD can be calculated as,

$$CDD_{daily} = T_{avg} - T_{base} \quad (1)$$

where CDD_{daily} is the daily CDD, T_{avg} is the daily average temperature calculated as an average of daily minimum and maximum temperatures, and T_{base} is the base temperature for calculating degree days which is typically 18°C or 65°F. The annual CDDs can be calculated by adding the daily CDDs throughout a year and it can be expressed as

$$CDD_{annual} = \sum_{i=1}^{365} CDD_{daily} \quad (2)$$

where CDD_{annual} are the annual cooling degree days for a particular year. Annual CDDs from both GHCN stations and NNR gridded data were calculated for the each year from 2008 through 2017 and their mean was used to calculate the long-term annual degree days.

Interpolation of Observed Cooling Degree Days

Cooling degree days from each station from the GHCN data were interpolated using geostatistical interpolation method of universal kriging (UK). Interpolation allows estimating the cooling degree days patterns in the highly impervious urban areas where the observational network is sparse. The interpolated cooling degree days are considered as the “observed” degree days since they are interpolated from the observed data from GHCN stations. NNR degree days are subtracted from the observed interpolated degree days to obtain the OMR cooling degree days to quantify the impacts from urbanization and other land-uses (Eugenia Kalnay and Cai 2003; L. Zhou et al. 2004; Ewing and Rong 2008; X. Yang, Hou, and Chen 2011). Using UK, the long-term mean annual CDDs from the stations was interpolated to $1 \text{ km} \times 1 \text{ km}$ grid resolution across CONUS. Geostatistical interpolation method such as UK is superior to ordinary least squares (OLS) interpolation. The OLS process requires the observations to be independent of each other and the residuals to be random and normally-distributed. However, temperature data are not independent of each other and temperature at one location is related to the temperature at nearby locations. Hence the residuals become correlated spatially (Chen et al. 2015). Since CDDs are calculated from temperature data, they also show spatial correlation and making OLS interpolation inapplicable here. UK was performed using two explanatory variables: percent imperviousness of the surface and elevation of the station. UK includes the spatial trends for interpolation and was introduced by Matheron (1969). The UK routine was performed using the “gstat” package (Gräler et al. 2016; Pebesma 2004) in the R-statistical software (R Core Team 2017). The UK method consists of a deterministic function, smoothly-varying and non-stationary trend, and a random function (Hengl and Toomanian 2006; L. Li, Romary, and Caers 2015; Mesić Kiš 2017). The smoothly-varying, non-stationary trend is known as the

drift, $\mu(x) \in \mathbb{R}$ and the independent zero-mean second order stationary residual random function $Y(x)$ that can be expressed as (Wackernagel 1998; L. Li, Romary, and Caers 2015; Mesić Kiš 2016; Mesić Kiš 2017):

$$Y(x) = Z(x) - \mu(x) \quad (3)$$

where $Z(x)$ is the predicted value at the locations where there is no samples. The expectation of the random function model, $\mu(x)$ varies spatially and is calculated by

$$\mu(x) = \sum_{l=0}^L \beta_l f_l(x) \quad (4)$$

where f_l are the unknown functions of spatial coordinates that describes the drift (or spatial trend, the tendencies of the values to change with the coordinates) and β_l are the coefficients. The kriging predictor Z^* of Z at location x_0 considering a linear trend of the sampled values can be expressed as

$$Z^*(x_0) = \sum_{i=1}^n \lambda_i Z(x_i) \quad (5)$$

where λ_i is the kriging weight at the observed location x_i considering unbiasedness and minimum variance. 80% of the total stations (randomly-selected) from GHCN were used in the model setup process and the rest 20% of the stations were used for the validation purpose.

To quantify the UHI impact on the CDDs, the observed minus reanalysis (OMR) method is used as described in the previous sections. Therefore, the differences in the interpolated and NNR degree days can be quantified as the UHI impact and it is calculated as

$$CDD \text{ difference} = CDD_{interp} - CDD_{NNR} \quad (6)$$

where CDD_{interp} is the interpolated long-term CDDs at grid level and CDD_{NNR} is the corresponding grid-level long-term mean CDDs from NNR. The OMR methodology is applicable for elevations lower 500 meters because the correlation between the observed and reanalysis temperature is low in the regions with elevations greater than 500 meters (Eugenia Kalnay and Cai 2003). For this reason, the study is limited to the urban areas with a mean elevation lower than 500 meters.

The UK prediction was evaluated using the observed CDDs at the randomly-selected stations that were not used in the model setup. The first statistics is bias which represents the systematic errors in the model and can be calculated as (Hengl, Heuvelink, and Stein 2004),

$$Bias = \frac{1}{n} \sum_{i=1}^n (Z^*(x) - Z(x)) \quad (7)$$

where n is the number of validation stations, $Z^*(x)$ is the predicted cooling degree days from the UK interpolation at the station location x and $Z(x)$ is the observed cooling degree days at the same station. To account for random errors, the root mean squared errors (RMSE) was calculated as,

$$RMSE = \sqrt{\frac{1}{n} \sum_{i=1}^n (Z^*(x) - Z(x))^2}. \quad (8)$$

Finally, the accuracy of the prediction was estimated from the normalized RMSE using the standard deviations of the observations,

$$RMSE_r = \frac{RMSE}{S_y} \quad (9)$$

where S_y is the standard deviation of the observations. If this normalized RMSE is less than 40%, then the estimated values are “fairly satisfactory.” If the value is greater than 71%, then the model accounts for less than 50% variability and the predictions are not considered satisfactory (Hengl, Heuvelink, and Stein 2004; Karl 2010).

Quantile Regression of Cooling Energy Intensity

Both RECS and CBECS data reported cooling energy consumption and floor area in the buildings. Also, RECS reported floor space used for cooling purposes (i.e., air-conditioning floor space). Cooling energy consumption intensity was calculated by dividing the cooling energy consumption by the corresponding floor area in each surveyed building (the cooling floor space for RECS data and the square footage of the building for CBECS data). The cooling energy consumption intensity was expressed in thousands BTU per square foot of the floor space. In addition, RECS and CBECS also provided weather-related information in the form of cooling degree days. Then a quantile regression estimation was established between cooling energy consumption intensity and several covariates including CDDs. Other covariates used in the study are building type (primary building activity for commercial buildings), the age of the building (i.e., the range of the year of construction), and the number of occupants in the building (i.e., household members for residential and number of employees for commercial building). To justify the use of quantile regression in the study, first regression diagnostics using ordinary least squares (OLS) were examined. First, the normality of the OLS residuals was checked for the regression between cooling energy consumption and the covariates using Shapiro-Wilk test diagnostics for normality

(Shapiro and Wilk 1965). The null hypothesis for the test statistics is the data is normally-distributed, and it is rejected when the p-value is lower than the selected level of significance. It has been found that, for all Census Divisions, the p-value of the Shapiro-Wilk test statistic is lower than the 1% significance level which led to the rejection of the null hypothesis of the data being normally-distributed. Therefore, OLS regression is inapplicable in this case, and a quantile regression is required which is used in the study with the covariates mentioned above. Among the covariates, building types and building construction year range are categorical variables. For each Census Division, different quantile regression was built between the cooling energy consumption intensity and the covariates. The raw survey data show that the variations in cooling energy consumption intensity increase with the increase in degree days in each Census Division. Hence OLS estimation is unable to capture such patterns in the data since it only captures the mean response of the dependent variable. Using the quantile regression approach, it is possible to capture such variations in the data and assess the uncertainty. It captures the response of the dependent variable at different quantile levels (i.e., conditional quantiles estimate) from the distribution of the entire dataset (Cade and Noon 2003; Koenker and Hallock 2001; Portnoy and Lin 2010). In addition to capturing differential response at the quantile levels, quantile regression is robust to outliers and non-normality in the data (Verkade et al. 2017). The weights corresponding to each surveyed building from the RECS and CBECS data were also considered in the quantile regression estimation. In each Census Division, quantile regression was performed at quantile levels of 0.05, 0.25, 0.50, 0.75, and 0.95 using the “quantreg” package (version 5.35) (Koenker 2018) in R-programming language (R Core Team 2017).

Floor Area Distribution and Total Energy Estimation

Total floor area from each Census Division was calculated using survey weights from the surveyed buildings. The disaggregation of the total floor area in each Census Division was performed using the proxy variable of grid-based population data. The disaggregation method from Righi et al. (2013) was applied in the study (Righi et al. 2013). Total population from each Census Division was also calculated from the after adding the gridded population. Then the per capita floor for each Census Division was calculated by dividing the total floor space and population. The per capita floor area was then multiplied by the population at each grid which eventually provides the floor area in each grid. The cooling energy consumption intensity was estimated from the CDDs and other covariates from UHI and non-UHI cases which were then multiplied by the gridded floor area to obtain the total cooling energy consumption at grid level. For other covariates than CDDs, a representative category of the variable was selected based on the frequency distribution of the variable. The most frequent category was selected for the categorical variables, while for the only other continuous variable of the number of occupants, the median value was selected. For residential buildings, the cooling energy consumption was calculated for single-family detached house types and the buildings made between 1970 and 1979 and for commercial buildings, the cooling energy consumption was calculated for office buildings and buildings made between 1980 and 1989. In addition, the cooling energy consumption contrasted with mobile homes and buildings made before 1950 for residential buildings and vacant buildings and buildings built before 1920 for commercial buildings. The median values for the occupancy were selected as two members for residential buildings and 19 employees for commercial buildings. These variables were kept constant, and only CDDs were varied for UHI and non-UHI cases to account for changes in CDDs due to UHI for the estimation of cooling energy

consumption. Therefore, cooling energy consumptions are compared against the contrasted variables and represent the representative building types, building construction year category, and the number of occupants.

UHI Impacts on Cooling Energy Consumption

CDDs estimation from UK method is referred to as the observed degree days and hence reflects the UHI case. Since the NNR data is not sensitive to surface characteristics, the NNR degree days are referred as the non-UHI case. Therefore, the differences in cooling energy consumption calculated from both UHI and non-UHI cases are the quantifications of impacts of UHI. The differences in cooling energy consumption between UHI and non-UHI cases were calculated in grid-levels and aggregated to the Census Division level from urban grids to quantify the UHI impacts.

CHAPTER 4. RESULTS AND DISCUSSION

Comparison between Observed and NNR Degree Days

First, the degree days observed in the GHCN stations and corresponding CDDs from NNR are compared with each other after resampling to the 1-km grid. The comparison is performed as a function of increasing imperviousness of the surface at the location of the GHCN stations. The increasing imperviousness of the surface indicates urbanization level from low- to high-density development. The comparison is presented in four categories of percent imperviousness of the surface: (1) less than 20% imperviousness, (2) 20 to 50% imperviousness, (3) 50 to 70% imperviousness, and (4) greater than 70% imperviousness.

The comparison for CDDs is shown in Figure 4.1. This figure shows the influence of UHI on long-term mean annual CDDs as a function of increasing imperviousness percentage. In this figure, the solid red line shows the slope of the best fit line and the black dashed line represents the 1:1 line. In Figure 4.1a, the value of the slope is 1.1 indicating that the long-term annual CDDs from GHCN and NNR are almost identical (i.e., the value of the slope is close to 1). In this figure, the values of surface imperviousness at the location of the stations are less than 20% which indicate the stations are located at low-density urban areas. The values of the slope increase with the increase in imperviousness of the surface (Figures 4.1b, c, and d). The values of the slope coefficients for imperviousness of the surface of 20%-50%, 50%-70%, and greater than 70% are 1.2, 1.3, and 1.5, respectively, which indicate that the observed CDDs can be up to 50% higher compared to NNR CDDs in the highly-developed area. The increasing values of the slope indicate there are more CDDs observed by the GHCN stations compared to the urbanization-insensitive NNR CDDs from low-density to high-density urban areas. Therefore, the differences between the long-term observed CDDs

by GHCN and NNR data can be attributed to surface characteristics including land-use change and urbanization (Eugenia Kalnay and Cai 2003). Therefore, the existence of UHI can be confirmed here since highly-built up areas raise the temperature (Clinton and Gong 2013; Xiaoma Li et al. 2017) and hence CDDs. The absence of vegetation in the highly-developed land areas lead to elevated temperature due to reduced evaporative cooling (D. Zhou et al. 2014; L. Zhao et al. 2014).

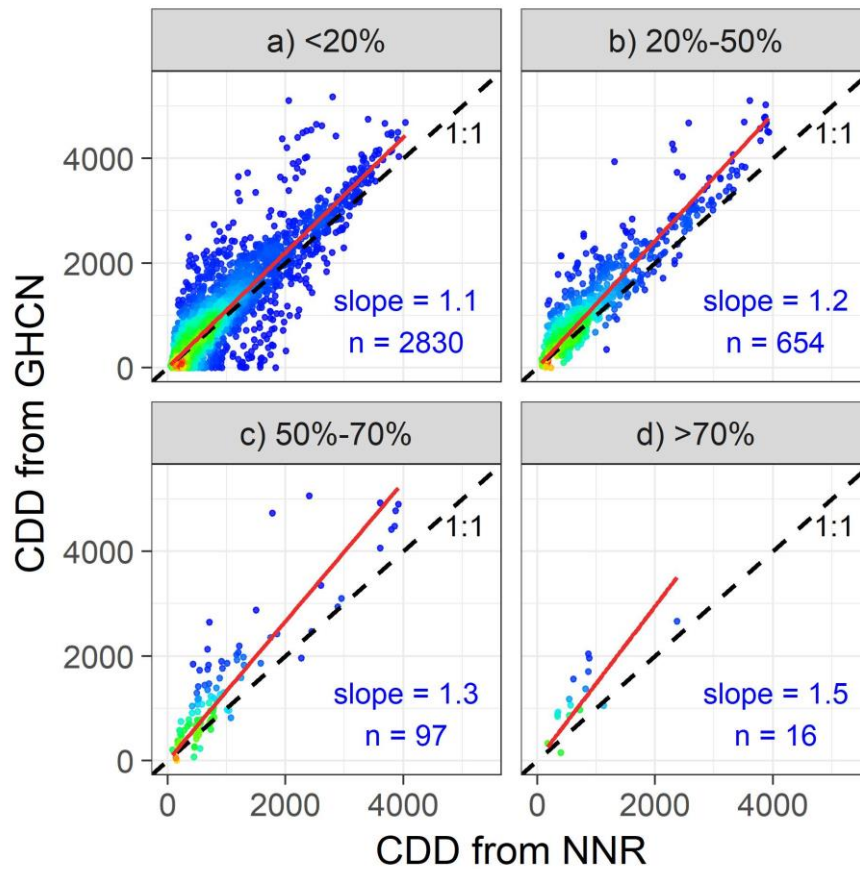


Figure 4.1: Relation between GHCN-observed and NNR CDDs [$^{\circ}\text{F}$] in imperviousness levels of a) less than 20%, b) from 20% to 50%, c) from 50% to 70%, and d) greater than 70% of imperviousness.

This figure also provides information about the availability of observational stations in the urban areas. Ground-based weather stations are usually situated in non-urban areas

with lower imperviousness of the surface, and they are scarce in the highly-developed urban areas. For example, there are 2,830 GHCN stations in the areas where the imperviousness of the surface lower than 20% and with increasing imperviousness the number of stations reduces. In the GHCN data, there are only 16 stations in locations with impervious surface areas greater than 70%. Therefore, fewer observations in the highly-developed urban areas limit the quantification of observed CDDs and necessitate the quantification of CDDs in such areas. It was accomplished using universal kriging, the results from which are presented in the following section.

Interpolation of CDDs using Universal Kriging

The degree days from the GHCN stations were interpolated to the grid-level using UK and the estimated degree days and the NNR degree days in the urban areas are shown in Figure 4.2a and Figure 4.2b. The general patterns in the degree days are similar in both figures. Warmer areas in the southern part have higher degree days compared to the northern areas which are much colder. To account for the UHI, the differences in CDDs from the estimated and NNR data are shown in the urban areas of the CONUS Figure 4.2c. The grids with differences greater than zero indicate that there are more CDDs observed than the urbanization-insensitive NNR CDDs and hence the impact of UHI. In the majority of the pixels in the urban areas in the CONUS, the difference is positive. The estimated difference between the observed CDDs and the NNR CDDs ranges between 250°F to 500°F in the northeastern part of the country, particularly near Mid Atlantic and New England Census Divisions that include major urban areas such as New York and Boston. These values are slightly higher than the values obtained by Landsberg (1981) for New York City using a pair of urban and rural stations during the period 1949-1970. These numbers are also higher than the CDD differences obtained by Rong (2006) for a different time period using the OMR

method that is used in this study. In the warmer western CONUS such as in California, these differences are much higher. In some of the urban grid areas in the region, the difference is higher than 1000°F CDDs. In the Los Angeles area, the differences start from 750 to greater than 1000°F CDDs. These values are also higher than the study by Landsberg (1981); however, the study period is between 1949-1970 using a pair of urban and rural stations. In the urban areas in South Atlantic and East South Central Census Divisions, the CDD difference ranges from 250°F to 750°F CDDs mostly. In Minneapolis, Minnesota, the spatial distribution of the CDD differences range mostly between 250°F and 500°F. These values are consistent with the values obtained by Todhunter (1996). The estimates for Toledo, Ohio are between 250°F and 500°F CDDs which are much lower than the values from the study by Schmidlin (1981). In Madison, Wisconsin, the CDD differences are less than 250°F which are lower than the values obtained in the study by Schatz and Kucharik (2016) using a network of 150 stations from 2012 to 2015. The OMR differences are higher in the states New York and Texas compared to the OMR differences calculated by Rong (2006). Nevertheless, the OMR differences in California are consistent with the differences found by Rong (2006). An opposite phenomenon is seen in the parts of the urban areas of the Midwestern and Southern United States in the parts of the South Atlantic, East North Central, West North Central, and West South Central Census Divisions. Several urban areas in these regions have lower observed CDDs compared to the NNR CDDs which resulted in a net cooling effect which is commonly referred to as urban cool islands. Such patterns are similar compared to the pattern seen in the study by Rong (2006) at station level using the OMR method. The study showed that, in the station locations in the Midwest near the Great Lakes and in the Southern parts of the country, the OMR difference is mostly negative and found

the OMR differences are insignificant in Florida. But that study used a different time period for the calculation of the long-term CDDs in observed and NNR CDDs. Zhao et al. (2014) mentioned that local background temperature plays a vital role in the UHI intensity. The UHI intensity is much lower in the regions with dry climate due to efficient convective cooling. Their study also found that the UHI intensity is much lower in these areas compared to the humid areas in the southeast and the east of the country. Urban greenspace and parks also contribute to the “cooling effect” in arid regions and hence lowering the UHI effect (L. Zhao et al. 2014). Other explanations of the “cooling effect” in these regions could be a reason of the urban layout, daytime cooling island effect, early morning advection urban canyons, and proximity to large water bodies and the Great Lakes for the Midwestern locations (Morris and Simmonds 2000; Rong 2006; Basara et al. 2008; H. Zhang, Jin, and Leach 2017). In Figure 4.2d, the OMR differences in the urban areas are shown in the relative frequency histogram. This histogram shows the occurrence of the OMR differences of CDDs relative to the total number of the pixels in urban areas lower than 500 meters. Positive values indicate the UHI effect using OMR and nearly 85.7% of the total pixels in the urban areas of the CONUS has positive values. The negative OMR differences correspond to the urban pixels in the Midwest and the Southern regions.

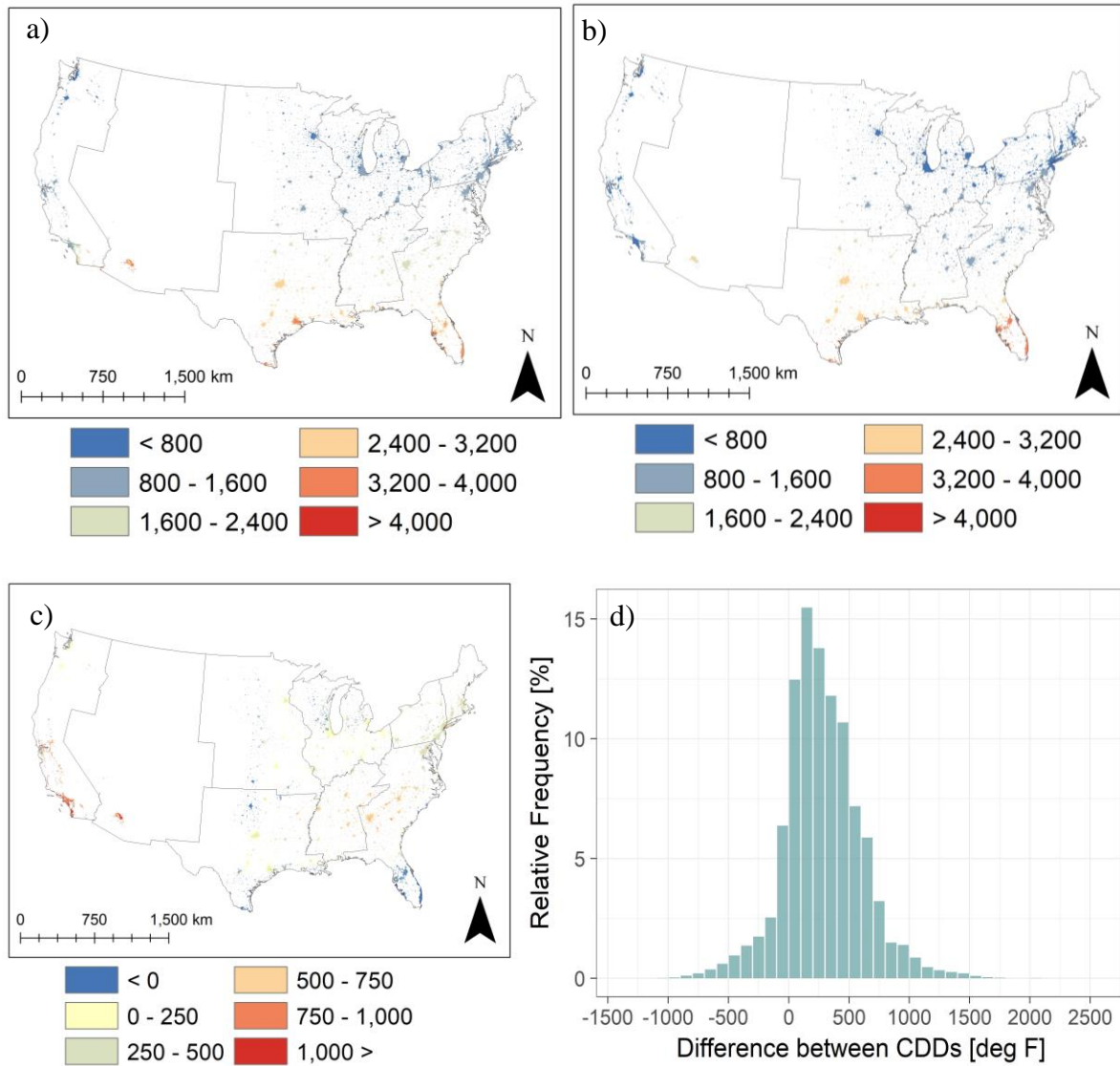


Figure 4.2: CDDs in the urban areas of CONUS, a) estimated from UK, b) NNR CDDs, c) differences in CDDs from UK and NNR, and d) the relative histogram of the differences in CDDs

The estimated cooling degree days were validated at the validation station locations which were not used in the UK predictions. The validation statistics used in the study are bias, $RMSE$, and $RMSE_r$. The calculated bias, $RMSE$, and $RMSE_r$ are -26.3°F , 347.1°F , and 0.3, respectively. The value of the $RMSE_r$ which shows the relative prediction error with

respect to the standard deviation are found to be 0.3 (Figure 4.3) which is less than 40%. The model predictions of CDDs are “fairly satisfactory” (Hengl, Heuvelink, and Stein 2004).

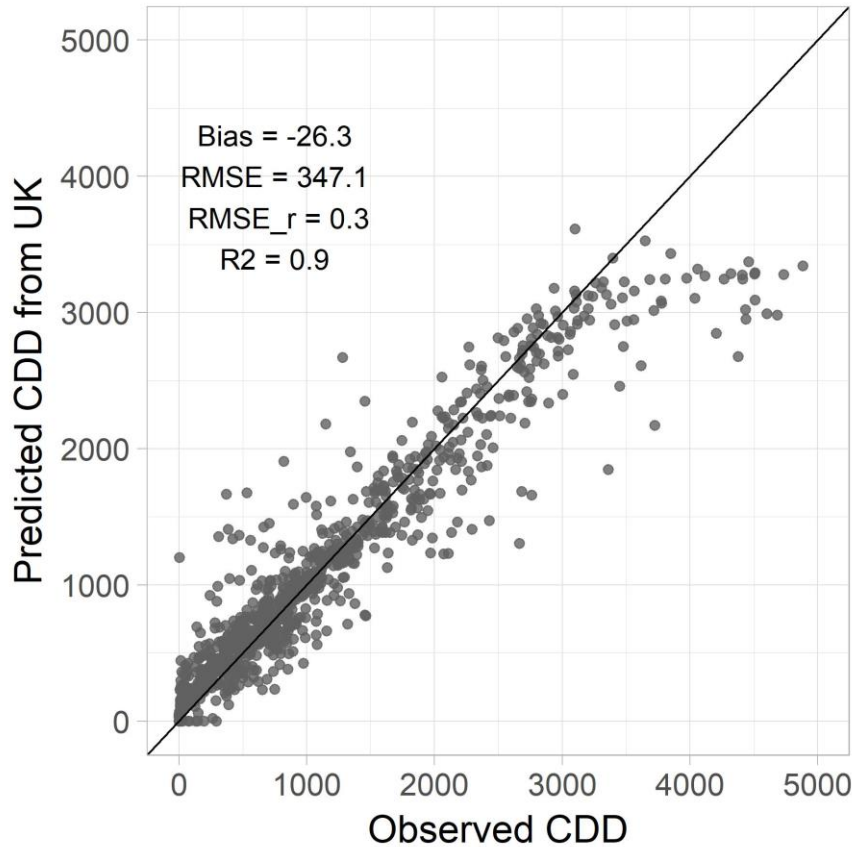


Figure 4.3: Validation statistics for predicted CDDs in °F

Quantile Regression Estimation of Cooling Energy Consumption

Cooling Energy Consumption Intensity with Cooling Degree Days

The variations in cooling energy consumption can be understood via quantile regression estimation. With the increasing cooling degree days, there is an increasing variation in cooling energy consumption. The variations are investigated via quantile regression method at quantile levels of 0.05, 0.25, 0.50, 0.75, and 0.95. Thus it represents the variations in cooling energy consumption intensity in a better way compared to the OLS regression using the mean response only (Kaza 2010). In Figure 4.4, the ranges of the slope

coefficients of cooling degree days from the quantile regression estimation are shown for different Census Divisions for both residential and commercial buildings. The ranges include the values of the slope coefficient from 0.05 to 0.95 quantile levels. The slope coefficients are estimated after using covariates such as building type, building construction year category, and occupancy in addition to the CDDs. The values of the slope coefficient are positive in all Census Divisions which indicate that with the increase in CDDs, there is an increase in cooling energy consumption. The lower end of the boxplot shows the value of the slope at 0.05 quantile level while the value at the upper end of the boxplot shows the value of the slope at 0.95 quantile level. For cooling energy consumption, the slope coefficients for median energy consumption intensity varies from 1.1×10^{-3} thousand BTU/sq.ft./CDD to 3.4×10^{-3} thousand BTU/sq.ft./CDD for residential buildings and 1.5×10^{-3} thousand BTU/sq.ft./CDD to 3.4×10^{-3} thousand BTU/sq.ft./CDD for commercial buildings in different Census Divisions. The slope value represents the change in cooling energy consumption intensity due to a unit change in degree days as a result of UHI (i.e., increase in CDDs). These values are much lower than the values obtained by Kaza (2010) using quantile regression. However, in that study, the slope represents energy use only because it used household size as one of the predictors in addition to other predictors including household types, neighborhood density, ownership of the household, year built, and annual income.

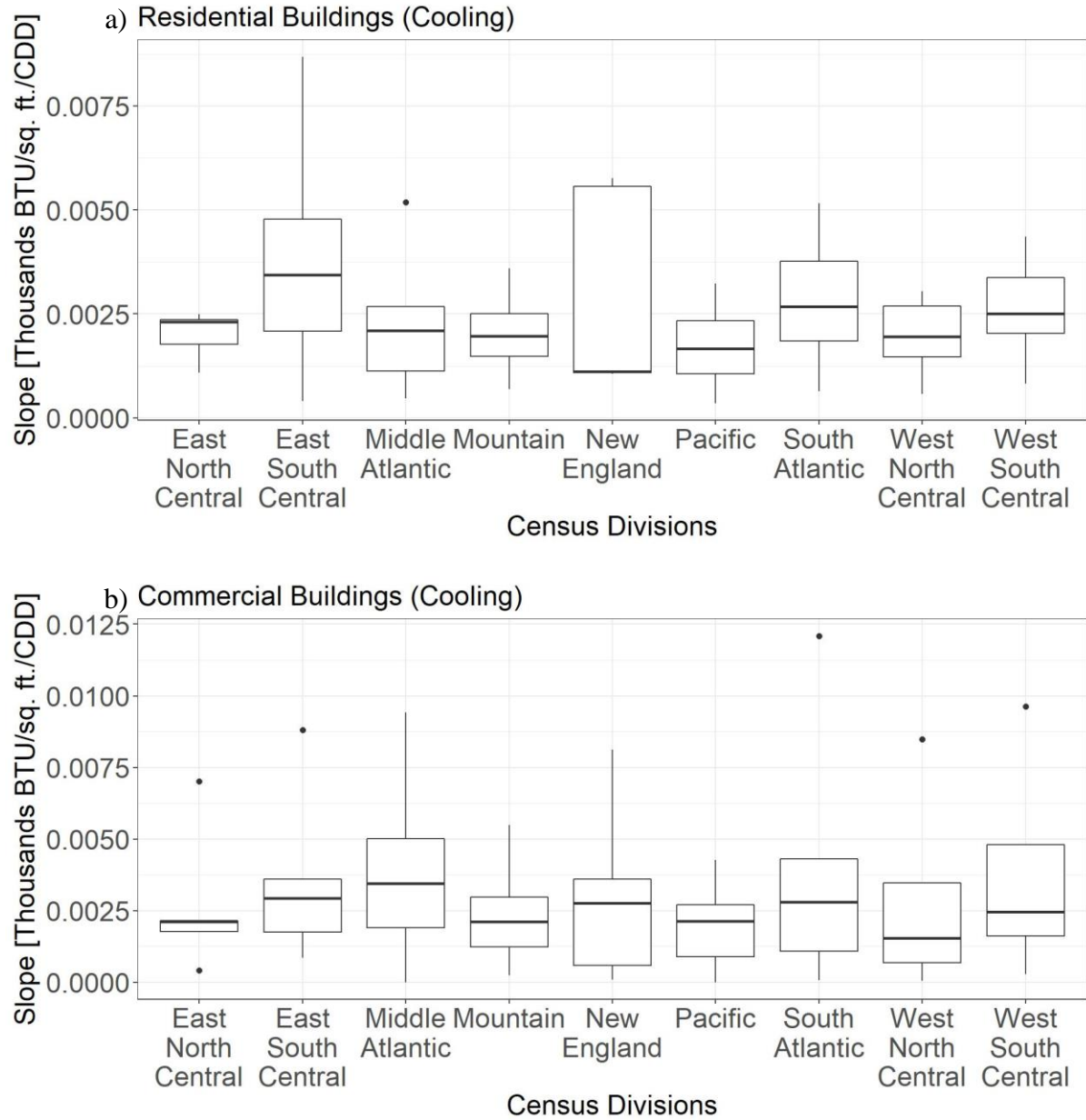


Figure 4.4: Slope coefficients of cooling energy consumption intensity from quantile regression at different Census Divisions for a) residential and b) commercial buildings

The boxplot in Figure 4.5 shows the variations of slope coefficients at each quantile level in all Census Division. The trends of the slopes in different quantile levels are very evident in the figure, i.e., with increasing quantile level, the values of the slope increases. The mean values of the slopes combining all Census Divisions at quantiles 0.05, 0.25, 0.50,

0.75, and 0.95 are summarized in Table 4.1. For example, the mean slopes in the residential buildings for the median quantile level is 2.1×10^{-3} thousand BTU/sq.ft./CDD. This value is almost half of the value that was found by Kaza (2010). He found that the slope for the median quantile as 4.8×10^{-3} thousand BTU per CDD for RECS data from 2005 using quantile regression including household factors in addition to CDDs. The mean value also indicates that 10 additional cooling degree days will cause an increase in cooling energy consumption by 21 BTU/sq.ft. on an average after controlling for other variables in residential buildings. The mean slope for median quantile level for commercial buildings is 2.5×10^{-3} thousand BTU/sq.ft./CDD which means 10 additional CDD will cause an increase in cooling energy consumption by 25 BTU/sq.ft.

There is a clear difference in cooling energy use intensity between the lowest and highest quantiles for cooling energy use. For commercial buildings in several Census Divisions, the slopes of the 0.05 quantile are nearly zero which indicate that the cooling energy consumption is not sensitive to CDD in these regions at this quantile level. The average slope coefficient from all Census Division at 0.95 quantile level is almost 37 times higher than the average slope coefficient from at 0.05 quantile level in commercial buildings. On the other hand, in residential buildings, the average slope coefficient for the 0.95 quantile level is nearly 6.7 times higher than the average slope coefficient for 0.05 quantile level. For a narrower quantile range, Kaza (2010) found a higher ratio. The study showed that cooling energy use at 0.9 quantile level is almost 8.5 times higher than the cooling energy use at 0.1 quantile level. These differences in slope coefficients at lowest to highest quantile levels confirm the non-constant variations in the cooling energy consumption in buildings with respect to CDDs. The non-constant variation is a result of the factors that were not taken into

account in the quantile regression (Cade and Noon 2003; Ewing and Rong 2008; Kaza 2010).

These factors include the socioeconomic and household-related factors such as occupant characteristics, household materials, behavior, income level, price, and others.

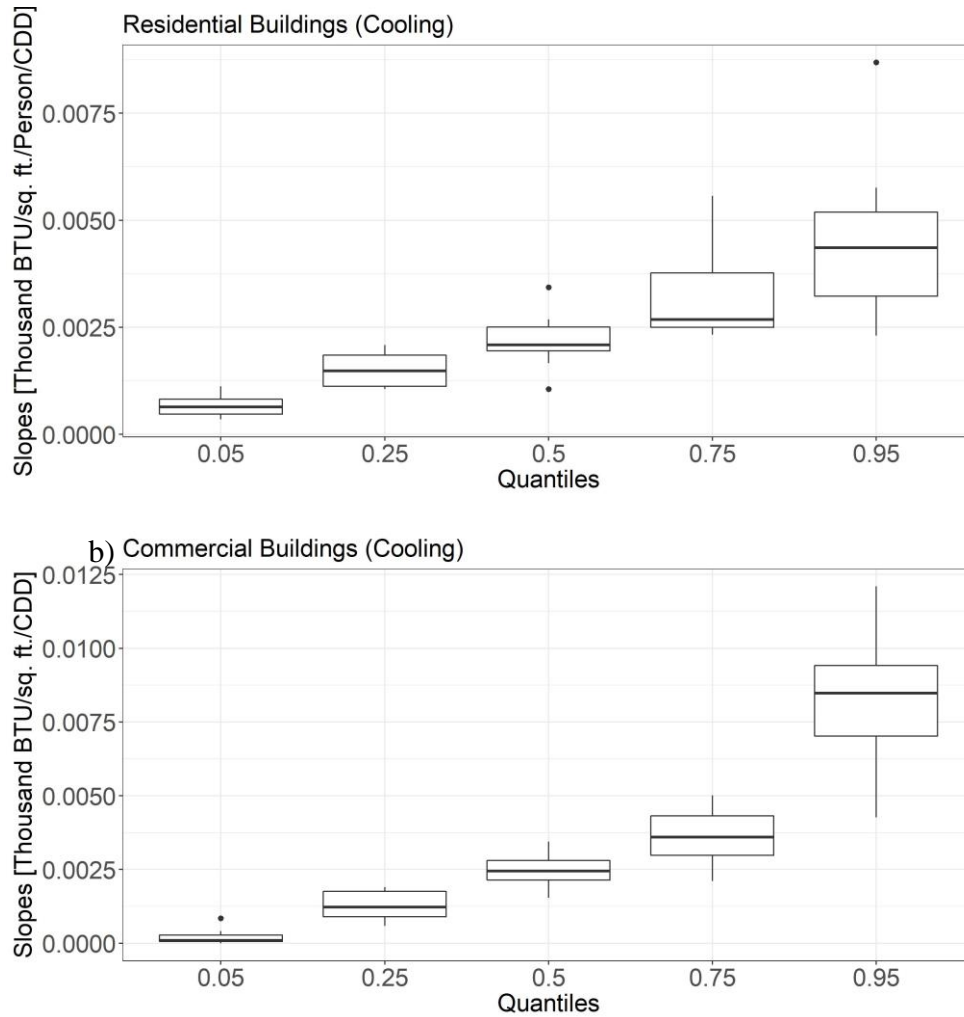


Figure 4.5: Variations in slopes at different quantile levels for the a) residential and b) commercial buildings

Table 4.1: Mean slope coefficients for cooling energy consumption (thousand BTU/sq.ft./CDD) in all Census Divisions at different quantile levels

Building Type	Slopes [$\times 10^{-3}$ thousand BTU/sq.ft./CDD]				
	0.05 Quantile	0.25 Quantile	0.50 Quantile	0.75 Quantile	0.95 Quantile
Residential	0.6	1.6	2.2	3.4	4.6
Commercial	0.2	1.3	2.5	3.6	8.1

Total Cooling Energy Consumption and the Impact of UHI

The energy consumptions for cooling for the median quantile are estimated for both UHI and Non-UHI cases holding other variables constant and they are added up to obtain the total cooling energy consumption in buildings. Also, the aggregated cooling energy consumption for 0.05 and 0.95 quantiles are estimated for each Census Division to estimate the complete range of cooling energy consumption from the lowest to highest quantile. As stated in the methodology section, the total cooling energy calculations only reflect cooling energy consumption in the selected building type, building construction year, and number of the occupant with contrast to the dummy variables for building type and building construction year. The cooling energy consumption and the impact of UHI are summarized for urban areas with a mean elevation of lower than 500 meters.

The spatial differences in median cooling energy consumption due to CDDs between UHI and non-UHI cases are shown in Figure 4.6. This figure shows that, the ranges for the differences in median cooling energy consumption is higher for commercial buildings. In the eastern CONUS, these differences are mostly ranged between 0% and 30% for residential buildings and between 25% and 75% for commercial buildings. The spatial distribution also

shows that UHI causes a higher increase in cooling energy consumption in the western part of the country in residential buildings compared to the commercial buildings. The negative differences in cooling energy consumptions correspond to the regions where UHI-related CDDs were found to be lower than the NNR CDDs. These regions are parts of the Midwest and South Atlantic region.

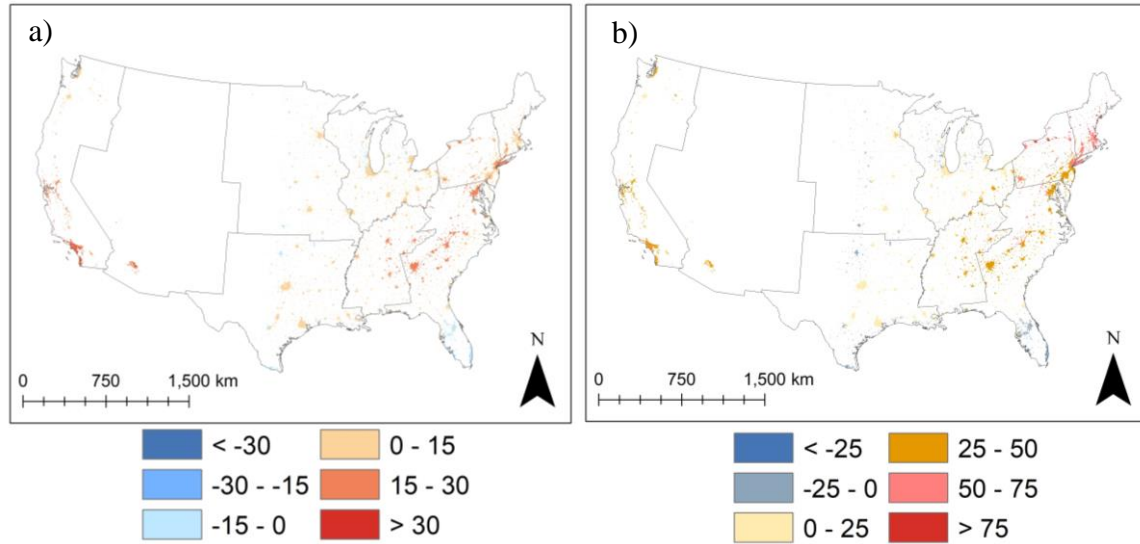


Figure 4.6: Percent differences in median cooling energy consumption for (a) residential buildings and (b) commercial buildings

Figure 4.7 shows the aggregated median cooling energy consumptions for the selected building type, building construction year, the number of occupants for UHI and non-UHI cases and their differences in each Census Division. The percent differences between aggregated cooling energy for UHI and non-UHI cases are shown in Figure 4.8. The aggregated cooling energy consumption in the Census Divisions for the UHI case in office buildings constructed between 1980 and 1989 with 19 employees ranges from 3.3×10^9 thousand BTU to 4.9×10^{10} thousand BTU. It ranges from 4.4×10^9 thousand BTU to 8.2×10^{10} thousand BTU for single-family detached house built between 1970 and 1979 with two occupants. The aggregated median cooling energy consumptions for UHI cases are

4.5% to 38.9% higher in residential buildings with a mean increase of 22.9% and 4.7% to 70.3% higher in commercial buildings with a mean increase of 28.1% in different Census Divisions when compared to the non-UHI cases. The mean values for residential and commercial buildings are close to the values obtained by Hirano and Fujita (2012) who used estimation equations between energy consumption and temperature. These values are slightly higher compared to the values found by Ojima (1991). There are four Census Divisions (East North Central, South Atlantic, West North Central, and West South Central) where the increase in cooling energy consumptions are close to the values obtained by Radhi and Sharples (2013) and C. Li et al. (2014). In residential buildings in the South Atlantic and West North Central Census Divisions, the percent increases in cooling energy consumption are closer to the values obtained by Fung et al. (2016). When comparing with the same study in commercial buildings, only in West North Central Census Division the percent increase in cooling energy consumption is closer to the value obtained by Fung et al. (2016). The percent increase in West North Central is also closer to the value obtained by Kolokotroni et al. (2012) for increase in cooling energy load in a model office building. The values in the South Atlantic Census Division are also consistent with the increase in cooling load by Cui et al. (2017). It is evident that UHI causes higher cooling energy consumption in the urban areas in all Census Divisions. The percent changes in cooling energy consumption as a result of UHI in both commercial and residential buildings are provided in Table 4.2. The ranges from the lowest to highest quantile are shown in the parentheses.

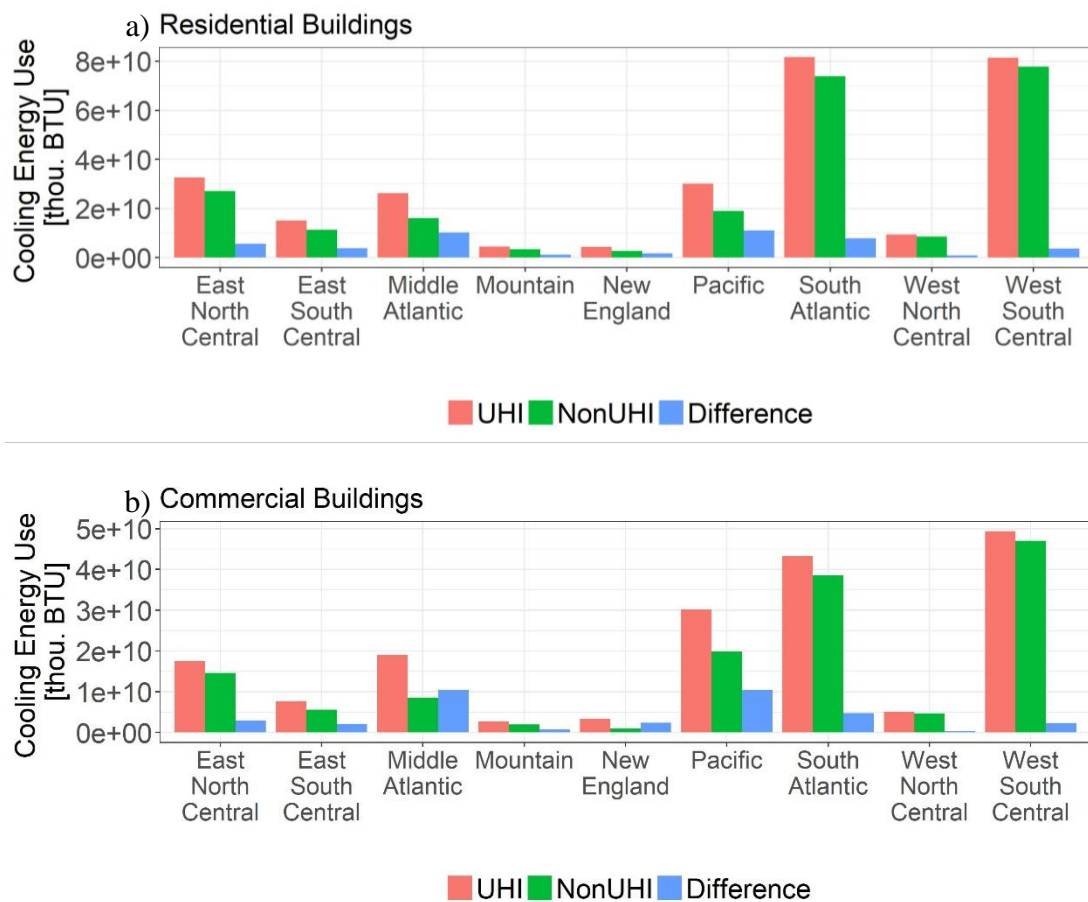


Figure 4.7: Cooling energy consumptions in (a) residential and (b) commercial buildings

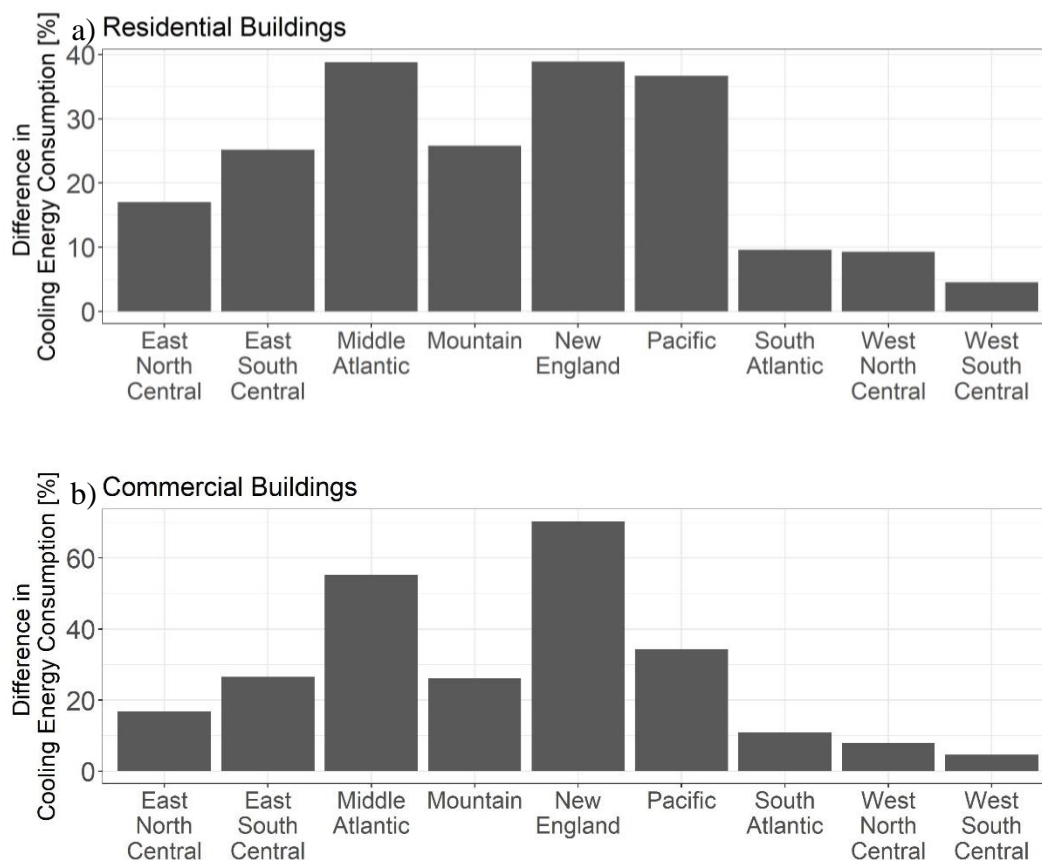


Figure 4.8: Percent differences in aggregated cooling energy use between UHI and non-UHI cases for (a) residential and (b) commercial buildings.

Table 4.2: Percent changes in median cooling energy use in all Census Divisions due to UHI (The ranges for 0.05-0.95 quantiles are given in the parentheses) holding other variables constant.

Census Divisions	Residential Buildings	Commercial Buildings
East North Central	17.0 (18.1-6.8)	16.8 (9.8-12.6)
East South Central	25.2 (13.4-18.0)	26.6 (16.6-29.2)
Middle Atlantic	38.8 (28.2-27.4)	55.2 (5.2-37.6)
Mountain	25.8 (32.3-19.8)	26.1 (16.3-26.7)
New England	38.9 (42.8-34.3)	70.3 (12.4-54.6)
Pacific	36.7 (26.8-34.3)	34.4 (5.0-20.3)
South Atlantic	9.6 (5.7-6.3)	11.0 (3.2-10.0)
West North Central	9.3 (6.8-4.4)	8.0 (1.8-9.7)
West South Central	4.5 (4.04-3.0)	4.7 (3.1-6.5)

CHAPTER 5. SUMMARY AND CONCLUSION

Summary of the Results

This study focuses on the urban heat island impact on the building energy consumption for cooling purposes. This study assesses how the increased temperature in urban areas impacts the cooling energy consumption in buildings by quantifying the cooling degree days in urban areas and the empirical relation between cooling energy consumption and cooling degree days and other variables.

To achieve the overarching goal of assessing the impact of UHI on building cooling energy consumption, this study addresses three research questions: (1) what are the impacts of UHI on observed CDDs? (2) How does cooling energy consumption relate to cooling degree days, and (3) what is the change in total cooling energy consumption in buildings as a result of additional CDDs due to UHI? The study first addresses the changes in CDDs due to increased urban temperatures. Using universal kriging, the observed CDDs are interpolated from the ground-based observational stations to urban grids and then compared with the urbanization-insensitive CDDs. First, the observed CDDs and the urbanization-insensitive CDDs were compared which showed that there are up to 50% higher cooling degree days due to increasing impervious surface in the urban areas. Results show that UHI can lead up to 2,509 additional cooling degree days at grid-level in the urban areas using universal kriging of the observed CDDs. Using quantile regression, the variations in energy consumption intensity with CDDs and other building characteristics such as type, age, and the number of occupants were observed in different Census Divisions. These results show that, on an average, one additional CDD will increase median cooling energy consumption by 2.1 BTU/sq.ft. in residential buildings and 2.5 BTU/sq.ft. in commercial buildings after

controlling for other variables. In the different Census Divisions of the United States, UHI causes an increase in median cooling energy consumption by 4.5% to 38.9% in residential buildings with an average increase of 22.9% and 4.7% to 70.3% in commercial buildings with an average increase of 28.1%.

Limitations and Future Directions

Although this study provides an estimation of cooling energy consumption in the buildings due to the UHI effects in the urban areas, it is noteworthy that building energy consumption does not solely depend on the ambient temperature. This study uses other variables such as building types, construction year, and the number of occupants. However, building materials and insulation play a crucial role in the building energy consumption and they vary in different regions based on climate zones. For example, buildings in the state of Massachusetts are well-insulated as a result of historical temperature patterns in the region (Amato et al. 2005). Although this study includes household characteristics such as building type, building construction year range, and occupancy in addition to weather-related variable of CDD, energy consumption is also dependent on other socioeconomic and building characteristics such as building size, orientation, building materials and their efficiencies, appliances, household income, urban sprawl, ownership status, and other variables (Ewing and Rong 2008; Kaza 2010). This study does not consider these factors in the computation of the building energy consumption since the primary focus of the study is on building energy consumption due to an elevated temperature from urban areas. The total cooling energy consumption and the corresponding increase due to UHI phenomena are presented for particular building types, the number of occupants, and building construction year. In addition to that, the energy consumption are contrasted with the dummy variables for building type and construction year. Therefore, the study does not represent the actual energy

consumption for all type of buildings, ages, and the number of occupants. The floor space data is estimated from the aggregated survey data and population distribution data. To compute the actual floor space, it is necessary to obtain building footprint and classification data from their actual location in space. The lack of such dataset led to the estimation of total cooling energy based on the population distribution data. The energy consumption data for residential and commercial buildings from the Energy Information Administration serves as a complete source of energy use data, but it has a limited sample size. It provides the location of the surveyed building as an administrative unit such as Census Division, but it does not provide any information on the climate zone which limits our understandings of the buildings energy consumption in response to the climate characteristics. Census Divisions are consist of several states and they include a wide range of climatic characteristics, particularly in the Mountain and Pacific Census Divisions. Also, the lower correlation between the observed and the NNR temperatures in the mountain areas limit our understandings of the UHI impacts in these regions, particularly in the Mountain Census Division. The Mountain Census Division included only a handful of urban clusters which may not be representative of the entire Census Division. Also, the Pacific Census Division includes Alaska and Hawaii in the RECS and CBECS dataset which may introduce bias in the estimation equations because their climates are different from that in the CONUS. This study could also serve as a preliminary step to further studies on urban heat island including building characteristics such as building type, age, and occupancy characteristics and incorporating building energy modeling software that takes into account different building characteristics and material types.

REFERENCES

- Ackerman, Bernice. 1985. "Temporal March of the Chicago Heat Island." *Journal of Climate and Applied Meteorology* 24.
- Akbari, Hashem, S. Davis, S. Dorsano, J. Huang, and S. Winert. 1992. "Cooling Our Communities - A Guidebook on Tree Planting and Light Colored Surfacing."
- Amato, Anthony D., Matthias Ruth, Paul Kirshen, and James Horwitz. 2005. "Regional Energy Demand Responses to Climate Change: Methodology and Application to the Commonwealth of Massachusetts." *Climatic Change* 71 (1-2): 175–201. doi:10.1007/s10584-005-5931-2.
- Arifwidodo, Sigit, and Orana Chandrasiri. 2015. "Urban Heat Island and Household Energy Consumption in Bangkok, Thailand." *Energy Procedia* 79. Elsevier B.V.: 189–94. doi:10.1016/j.egypro.2015.11.461.
- Atkinson, B. W. 2003. "Numerical Modelling of Urban Heat-Island Intensity." *Boundary-Layer Meteorology* 109 (3). Kluwer Academic Publishers: 285–310. doi:10.1023/A:1025820326672.
- Azevedo, Juliana Antunes, Lee Chapman, and Catherine L. Muller. 2016. "Urban Heat and Residential Electricity Consumption: A Preliminary Study." *Applied Geography* 70. Elsevier Ltd: 59–67. doi:10.1016/j.apgeog.2016.03.002.
- Bagiorgas, H. S., and G. Mihalakakou. 2016. "On the Influence of the Urban Heat Island on the Cooling Load of a School Building in Athens, Greece." *Journal of Atmospheric and Solar-Terrestrial Physics* 138-139. Elsevier: 179–86. doi:10.1016/j.jastp.2016.01.002.
- Basara, Jeffrey B., Peter K. Hall, Amanda J. Schroeder, Bradley G. Illston, and Kodi L. Nemunaitis. 2008. "Diurnal Cycle of the Oklahoma City Urban Heat Island." *Journal of Geophysical Research Atmospheres* 113 (20): 1–16. doi:10.1029/2008JD010311.
- Berger, Tania, Christof Amann, Herbert Formayer, Azra Korjenic, Bernhard Pospichal, Christoph Neururer, and Roman Smutny. 2014. "Impacts of Urban Location and Climate Change upon Energy Demand of Office Buildings in Vienna, Austria." *Building and Environment* 81. Elsevier Ltd: 258–69. doi:10.1016/j.buildenv.2014.07.007.
- Bokaie, Mehdi, Mirmasoud Kheirkhah Zarkesh, Peyman Daneshkar Arasteh, and Ali Hosseini. 2016. "Assessment of Urban Heat Island Based on the Relationship between Land Surface Temperature and Land Use/Land Cover in Tehran." *Sustainable Cities and Society* 23. Elsevier B.V.: 94–104. doi:http://dx.doi.org/10.1016/j.scs.2016.03.009.
- Brown, Marilyn A., Matt Cox, Ben Staver, and Paul Baer. 2015. "Modeling Climate-Driven Changes in U.S. Buildings Energy Demand." *Climatic Change* 134 (1-2): 29–44. doi:10.1007/s10584-015-1527-7.

- Cade, Brian S., and Barry R. Noon. 2003. "A Gentle Introduction to Quantile Regression for Ecologists." *Frontiers in Ecology and the Environment* 1 (8): 412–20. doi:10.1890/1540-9295(2003)001[0412:AGITQR]2.0.CO;2.
- Charabi, Yassine, and Abdelhamid Bakhit. 2011. "Assessment of the Canopy Urban Heat Island of a Coastal Arid Tropical City: The Case of Muscat, Oman." *Atmospheric Research* 101 (1-2): 215–27. doi:10.1016/j.atmosres.2011.02.010.
- Chen, Fengrui, Yu Liu, Qiang Liu, and Fen Qin. 2015. "A Statistical Method Based on Remote Sensing for the Estimation of Air Temperature in China." *International Journal of Climatology* 35 (8): 2131–43. doi:10.1002/joc.4113.
- Chun, B., and J. M. Guldmann. 2014. "Spatial Statistical Analysis and Simulation of the Urban Heat Island in High-Density Central Cities." *Landscape and Urban Planning* 125. Elsevier B.V.: 76–88. doi:10.1016/j.landurbplan.2014.01.016.
- Clinton, Nicholas, and Peng Gong. 2013. "MODIS Detected Surface Urban Heat Islands and Sinks: Global Locations and Controls." *Remote Sensing of Environment* 134. Elsevier Inc.: 294–304. doi:10.1016/j.rse.2013.03.008.
- Cui, Ying, Da Yan, Tianzhen Hong, and Jingjin Ma. 2017. "Temporal and Spatial Characteristics of the Urban Heat Island in Beijing and the Impact on Building Design and Energy Performance." *Energy* 130. Elsevier Ltd: 286–97. doi:10.1016/j.energy.2017.04.053.
- DOE2. 2008. "eQuest: The Quick Energy Simulation Tool." www.doe2.com.
- Easterling, David R., Briony Horton, Philip D. Jones, Thomas C. Peterson, Thomas R. Karl, David E. Parker, M. J. Salinger, et al. 1997. "Maximum and Minimum Temperature Trends for the Globe." *Science* 277 (5324). American Association for the Advancement of Science: 364–67. doi:10.1126/science.277.5324.364.
- EIA. 2018. "Monthly Energy Review: April 2018." Washington, DC.
- Ewing, Reid, and Fang Rong. 2008. "The Impact of Urban Form on U.S. Residential Energy Use." *Housing Policy Debate* 19 (1). Taylor & Francis Group: 1–30. doi:10.1080/10511482.2008.9521624.
- Fortuniak, K., Kazimierz Kłysik, and J. Wibig. 2006. "Urban-Rural Contrasts of Meteorological Parameters in Łódź." *Theoretical and Applied Climatology* 84: 91–101.
- Fung, W. Y., K. S. Lam, W. T. Hung, S. W. Pang, and Y. L. Lee. 2006. "Impact of Urban Temperature on Energy Consumption of Hong Kong." *Energy* 31 (14): 2287–2301. doi:10.1016/j.energy.2005.12.009.
- Gallo, K.P., T.W. Owen, D.R. Easterling, and P. F. Jamason. 1999. "Temperature Trends of the U . S . Historical Climatology Network Based on Satellite-Designated Land Use/

- Land Cover.” *Papers in Natural Resources* 12: 1344–48. doi:10.1175/1520-0442(1999)012<1344:TTOTUS>2.0.CO;2.
- Gallo, Kevin P., David R. Easterling, and Thomas C. Peterson. 1996. “The Influence of Land Use/Land Cover on Climatological Values of the Diurnal Temperature Range.” *Journal of Climate* 9 (11): 2941–44. doi:10.1175/1520-0442(1996)009<2941:TIOLUC>2.0.CO;2.
- Goward, Samuel N. 1981. “Thermal Behavior of Urban Landscapes and the Urban Heat Island.” *Phys Geogr* 2 (1): 19–33.
- Gräler, Benedikt, Edzer Pebesma, Gerard Heuvelink, and Benedikt Gräler. 2016. “Spatio-Temporal Interpolation Using Gstat.” *The R Journal* 8 (1): 204–18. doi:10.1007/978-3-319-17885-1.
- Hansen, J, R Ruedy, and M Sato. 2001. “A Closer Look at United States and Global Surface Temperature Change.” *Journal of Geophysical Research* 106 (D20): 947–63.
- Heinl, Michael, Albin Hammerle, Ulrike Tappeiner, and Georg Leitinger. 2015. “Determinants of Urban-Rural Land Surface Temperature Differences - A Landscape Scale Perspective.” *Landscape and Urban Planning* 134. Elsevier B.V.: 33–42. doi:10.1016/j.landurbplan.2014.10.003.
- Heiple, Shem, and David J. Sailor. 2008. “Using Building Energy Simulation and Geospatial Modeling Techniques to Determine High Resolution Building Sector Energy Consumption Profiles.” *Energy and Buildings* 40 (8): 1426–36. doi:10.1016/j.enbuild.2008.01.005.
- Hengl, Tomislav, Gerard B M Heuvelink, and Alfred Stein. 2004. “A Generic Framework for Spatial Prediction of Soil Variables Based on Regression-Kriging.” *Geoderma* 120 (1-2): 75–93. doi:10.1016/j.geoderma.2003.08.018.
- Hengl, Tomislav, and Norair Toomanian. 2006. “Maps Are Not What They Seem : Representing Uncertainty in Soil- Property Maps.” *Spatial Accuracy Assessment in Natural Resources and Environmental Sciences*, 805–13.
- Hirano, Y., and T. Fujita. 2012. “Evaluation of the Impact of the Urban Heat Island on Residential and Commercial Energy Consumption in Tokyo.” *Energy* 37 (1): 371–83. doi:10.1016/j.energy.2011.11.018.
- Homer, C.G., J.A. Dewitz, L. Yang, S. Jin, P. Danielson, G. Xian, J. Coulston, N.D. Herold, J.D. Wickham, and K. Megown. 2015. “Completion of the 2011 National Land Cover Database for the Conterminous United States-Representing a Decade of Land Cover Change Information.” *Photogrammetric Engineering and Remote Sensing* 81 (5): 345–54. doi:10.14358/PERS.81.5.345.

- Howard, B., L. Parshall, J. Thompson, S. Hammer, J. Dickinson, and V. Modi. 2012. "Spatial Distribution of Urban Building Energy Consumption by End Use." *Energy and Buildings* 45. Elsevier B.V.: 141–51. doi:10.1016/j.enbuild.2011.10.061.
- Hu, Xiao Ming, Ming Xue, Petra M. Klein, Bradley G. Illston, and Sheng Chen. 2016. "Full Access Analysis of Urban Effects in Oklahoma City Using a Dense Surface Observing Network." *Journal of Applied Meteorology and Climatology* 55 (3): 723–41. doi:10.1175/JAMC-D-15-0206.1.
- Huang, Weijiao, Jun Li, Qiaoying Guo, Lamin R. Mansaray, Xinxing Li, and Jingfeng Huang. 2017. "A Satellite-Derived Climatological Analysis of Urban Heat Island over Shanghai during 2000-2013." *Remote Sensing* 9 (7): 1–27. doi:10.3390/rs9070641.
- Imhoff, Marc L., Ping Zhang, Robert E. Wolfe, and Lahouari Bounoua. 2010. "Remote Sensing of the Urban Heat Island Effect across Biomes in the Continental USA." *Remote Sensing of Environment* 114 (3): 504–13. doi:10.1016/j.rse.2009.10.008.
- Isaac, Morna, and Detlef P. van Vuuren. 2009. "Modeling Global Residential Sector Energy Demand for Heating and Air Conditioning in the Context of Climate Change." *Energy Policy* 37: 507–21. doi:10.1016/j.enpol.2008.09.051.
- Jingyong, Zhang, Dong Wenjie, Wu Lingyun, Wei Jiangfeng, Chen Peiyan, and Dong-Kyou Lee. 2005. "Impact of Land Use Changes on Surface Warming in China." *Advances in Atmospheric Sciences* 22 (3): 343–48. doi:10.1007/BF02918748.
- Jones, P. D., D. H. Lister, and Q. Li. 2008. "Urbanization Effects in Large-Scale Temperature Records, with an Emphasis on China." *Journal of Geophysical Research Atmospheres* 113 (16): 1–12. doi:10.1029/2008JD009916.
- Kalnay, E., M. Kanamitsu, R. Kistler, W. Collins, D. Deaven, L. Gandin, M. Iredell, et al. 1996. "The NCEP/NCAR 40-Year Reanalysis Project." *Bulletin of the American Meteorological Society* 77 (3): 437–71. doi:10.1175/1520-0477(1996)077<0437:TNYRP>2.0.CO;2.
- Kalnay, Eugenia, and Ming Cai. 2003. "Impact of Urbanization and Land-Use Change on Climate." *Nature* 423 (6939): 528–31.
- Kalnay, Eugenia, Ming Cai, Hong Li, and Jayakar Tobin. 2006. "Estimation of the Impact of Land-Surface Forcings on Temperature Trends in Eastern United States." *Journal of Geophysical Research Atmospheres* 111 (6): 1–13. doi:10.1029/2005JD006555.
- Karl, Jason W. 2010. "Spatial Predictions of Cover Attributes of Rangeland Ecosystems Using Regression Kriging and Remote Sensing." *Rangeland Ecology & Management* 63 (3). Elsevier: 335–49. doi:10.2111/REM-D-09-00074.1.
- Kaza, Nikhil. 2010. "Understanding the Spectrum of Residential Energy Consumption: A Quantile Regression Approach." *Energy Policy* 38 (11). Elsevier: 6574–85. doi:10.1016/j.enpol.2010.06.028.

- Kikegawa, Yukihiro, Yutaka Genchi, Hiroshi Yoshikado, and Hiroaki Kondo. 2003. "Development of a Numerical Simulation System toward Comprehensive Assessments of Urban Warming Countermeasures Including Their Impacts upon the Urban Buildings' Energy-Demands." *Applied Energy* 76 (4): 449–66. doi:10.1016/S0306-2619(03)00009-6.
- Kim, Yeon-Hee, and Jong-Jin Baik. 2005. "Spatial and Temporal Structure of the Urban Heat Island in Seoul." *Journal of Applied Meteorology* 44 (5): 591–605. doi:10.1175/JAM2226.1.
- Ko, Yekang. 2013. "Urban Form and Residential Energy Use: A Review of Design Principles and Research Findings." *Journal of Planning Literature* 28 (4): 327–51. doi:10.1177/0885412213491499.
- Koenker, Roger W. 2018. "Quantreg: Quantile Regression. R Package Version 5.35." <https://cran.r-project.org/package=quantreg>.
- Koenker, Roger W, and Kevin F Hallock. 2001. "Quantile Regression." *Journal of Economic Perspectives* 15 (4): 143–56.
- Kolokotroni, M., X. Ren, M. Davies, and A. Mavrogianni. 2012. "London's Urban Heat Island: Impact on Current and Future Energy Consumption in Office Buildings." *Energy and Buildings* 47. Elsevier B.V.: 302–11. doi:10.1016/j.enbuild.2011.12.019.
- Kolokotroni, Maria, Yuepeng Zhang, and Richard Watkins. 2007. "The London Heat Island and Building Cooling Design." *Solar Energy* 81 (1): 102–10. doi:10.1016/j.solener.2006.06.005.
- Laboratory, Solar Energy. 1997. "University of Wisconsin and Transsolar Stuttgart: TRNSYS Version 14-A Transient System Simulation Program."
- Lam, Joseph C. 1998. "Climatic and Economic Influences on Residential Electricity Consumption." *Energy Conversion and Management* 39 (7): 623–29. doi:10.1016/S0196-8904(97)10008-5.
- Landsberg, H E. 1981. *The Urban Climate*. International Geophysics. Elsevier Science. <https://books.google.com/books?id=zKkHiEXZGBIC>.
- Lawrimore, Jay H., Matthew J. Menne, Byron E. Gleason, Claude N. Williams, David B. Wuertz, Russell S. Vose, and Jared Rennie. 2011. "An Overview of the Global Historical Climatology Network Monthly Mean Temperature Data Set, Version 3." *Journal of Geophysical Research Atmospheres* 116 (19): 1–18. doi:10.1029/2011JD016187.
- Li, Canbing, Jinju Zhou, Yijia Cao, Jin Zhong, Yu Liu, Chongqing Kang, and Yi Tan. 2014. "Interaction between Urban Microclimate and Electric Air-Conditioning Energy Consumption during High Temperature Season." *Applied Energy* 117. Elsevier Ltd: 149–56. doi:10.1016/j.apenergy.2013.11.057.

- Li, Lewis, Thomas Romary, and Jef Caers. 2015. "Universal Kriging with Training Images." *Spatial Statistics* 14. Elsevier Ltd: 240–68. doi:10.1016/j.spasta.2015.04.004.
- Li, Wenliang, Yuyu Zhou, Kristen Cetin, Jiyong Eom, Yu Wang, Gang Chen, and Xuesong Zhang. 2017. "Modeling Urban Building Energy Use: A Review of Modeling Approaches and Procedures." *Energy* 141. Elsevier Ltd: 2445–57. doi:10.1016/j.energy.2017.11.071.
- Li, Xiaoma, Yuyu Zhou, Ghassem R. Asrar, Marc Imhoff, and Xuecao Li. 2017. "The Surface Urban Heat Island Response to Urban Expansion: A Panel Analysis for the Conterminous United States." *Science of the Total Environment* 605–606. Elsevier B.V.: 426–35. doi:10.1016/j.scitotenv.2017.06.229.
- Li, Xiaoxiao, Wenwen Li, A. Middel, S.L. Harlan, A.J. Brazel, and B.L. Turner. 2016. "Remote Sensing of the Surface Urban Heat Island and Land Architecture in Phoenix, Arizona: Combined Effects of Land Composition and Configuration and Cadastral–demographic–economic Factors." *Remote Sensing of Environment* 174 (March): 233–43. doi:10.1016/j.rse.2015.12.022.
- Liao, Weilin, Xiaoping Liu, Dagang Wang, and Yanling Sheng. 2017. "The Impact of Energy Consumption on the Surface Urban Heat Island in China's 32 Major Cities." *Remote Sensing* 9 (3). doi:10.3390/rs9030250.
- Lundgren, Karin, and Tord Kjellstrom. 2013. "Sustainability Challenges from Climate Change and Air Conditioning Use in Urban Areas." *Sustainability (Switzerland)* 5 (7): 3116–28. doi:10.3390/su5073116.
- Magli, Susanna, Chiara Lodi, Luca Lombroso, Alberto Muscio, and Sergio Teggi. 2015. "Analysis of the Urban Heat Island Effects on Building Energy Consumption." *International Journal of Energy and Environmental Engineering* 6 (1): 91–99. doi:10.1007/s40095-014-0154-9.
- Matheron, G. 1969. "Le Krigeage Universel. In: Fontainebleau: Cahiers Du Center de Morphologie Mathématique." École des Mines de Paris.
- Menberg, Kathrin, Philipp Blum, Axel Schaffitel, and Peter Bayer. 2013. "Long-Term Evolution of Anthropogenic Heat Fluxes into a Subsurface Urban Heat Island." *Environmental Science and Technology* 47 (17): 9747–55. doi:10.1021/es401546u.
- Menne, Matthew J., Imke Durre, Russell S. Vose, Byron E. Gleason, and Tamara G. Houston. 2012. "An Overview of the Global Historical Climatology Network-Daily Database." *Journal of Atmospheric and Oceanic Technology* 29 (7): 897–910. doi:10.1175/JTECH-D-11-00103.1.
- Mesić Kiš, Ivana. 2016. "Comparison of Ordinary and Universal Kriging Interpolation Techniques on a Depth Variable (a Case of Linear Spatial Trend) , Case Study of the Šandrovac Field." *The Mining-Geology-Petroleum Engineering Bulletin*, 41–58. doi:10.17794/rgn.2016.2.4.

- . 2017. “Contribution To Terminology and Application of New Geostatistical Mapping Methods in Croatia - Universal Kriging.” *Rudarsko-Geološko-Naftni Zbornik* 32 (4): 31–35. doi:10.17794/rgn.2017.4.3.
- Min, Jihoon, Zeke Hausfather, and Qi Feng Lin. 2010. “A High-Resolution Statistical Model of Residential Energy End Use Characteristics for the United States.” *Journal of Industrial Ecology* 14 (5): 791–807. doi:10.1111/j.1530-9290.2010.00279.x.
- Morris, C. J G, and I. Simmonds. 2000. “Associations between Varying Magnitudes of the Urban Heat Island and the Synoptic Climatology in Melbourne, Australia.” *International Journal of Climatology* 20 (15): 1931–54. doi:10.1002/1097-0088(200012)20:15<1931::AID-JOC578>3.0.CO;2-D.
- Ojima, T. 1991. “Changing Tokyo Metropolitan Area and Its Heat Island Model.” *Energy and Buildings* 15 (1-2): 191–203.
- Oke, T. R. 1973. “City Size and the Urban Heat Island.” *Atmospheric Environment Pergamon Press* 7: 769–79. doi:10.1016/0004-6981(73)90140-6.
- . 1987. *Boundary Layer Climates*. Second. Methuen and Co. Ltd.
- Oke, T. R., and G. B. Maxwell. 1975. “Urban Heat Island Dynamics in Montreal and Vancouver.” *Atmospheric Environment (1967)* 9 (2): 191–200. doi:10.1016/0004-6981(75)90067-0.
- Pebesma, Edzer J. 2004. “Multivariable Geostatistics in S: The Gstat Package.” *Computers & Geosciences* 30: 683–91.
- Peng, S S, S L Piao, P Ciais, P Friedlingstein, C Otle, F M Breon, H J Nan, L M Zhou, and R B Myneni. 2012. “Surface Urban Heat Island Across 419 Global Big Cities.” *Environmental Science & Technology* 46 (2): 696–703. doi:Doi 10.1021/Es2030438.
- Portnoy, Stephen, and Guixian Lin. 2010. “Asymptotics for Censored Regression Quantiles.” *Journal of Nonparametric Statistics* 22 (1): 115–30. doi:10.1080/10485250903105009.
- R Core Team. 2017. “R: A Language and Environment for Statistical Computing.” Vienna, Austria. <https://www.r-project.org/>.
- Radhi, Hassan, and Stephen Sharples. 2013. “Quantifying the Domestic Electricity Consumption for Air-Conditioning due to Urban Heat Islands in Hot Arid Regions.” *Applied Energy* 112. Elsevier Ltd: 371–80. doi:10.1016/j.apenergy.2013.06.013.
- Righi, S., F. Farina, S. Marinello, M. Andretta, P. Luciali, and E. Pollini. 2013. “Development and Evaluation of Emission Disaggregation Models for the Spatial Distribution of Non-Industrial Combustion Atmospheric Pollutants.” *Atmospheric Environment* 79. Elsevier Ltd: 85–92. doi:10.1016/j.atmosenv.2013.06.021.

- Rizwan, Ahmed Memon, Leung Y. C. Dennis, and Chunho Liu. 2008. "A Review on the Generation, Determination and Mitigation of Urban Heat Island." *Journal of Environmental Sciences* 20 (1): 120–28. doi:10.1016/S1001-0742(08)60019-4.
- Rong, Fang. 2006. "Impact of Urban Sprawl on US Residential Energy Use."
- Sailor, David J. 2001. "Relating Residential and Commercial Sector Electricity Loads to Climate - Evaluating State Level Sensitivities and Vulnerabilities." *Energy* 26 (7): 645–57. doi:10.1016/S0360-5442(01)00023-8.
- Santamouris, M, N Papanikolaou, I Livada, I Koronakis, C Georgakis, A Argiriou, and D. N. Assimakopoulos. 2001. "On the Impact of Urban Climate on the Energy Consumption of Buildings." *Solar Energy* 70 (3): 201–16. doi:10.1016/S0038-092X(00)00095-5.
- Santamouris, Mat. 2007. "Heat Island Research in Europe: The State of the Art." *Advances in Building Energy Research* 1 (1): 123–50. doi:10.1080/17512549.2007.9687272.
- Santamouris, Mat, Shamila Haddad, Francesco Fiorito, Paul Osmond, Lan Ding, Deo Prasad, Xiaoqiang Zhai, and Ruzhu Wang. 2017. "Urban Heat Island and Overheating Characteristics in Sydney, Australia. An Analysis of Multiyear Measurements." *Sustainability (Switzerland)* 9 (5). doi:10.3390/su9050712.
- Schatz, Jason, and Christopher J. Kucharik. 2014. "Seasonality of the Urban Heat Island Effect in Madison, Wisconsin." *Journal of Applied Meteorology and Climatology* 53 (10): 2371–86. doi:10.1175/JAMC-D-14-0107.1.
- . 2016. "Urban Heat Island Effects on Growing Seasons and Heating and Cooling Degree Days in Madison, Wisconsin USA." *International Journal of Climatology* 36 (15): 4873–84. doi:10.1002/joc.4675.
- Schmidlin, T. W. 1981, "The urban heat island at Toledo, Ohio." *The Ohio Journal of Science*. **89** (3): 38-41
- Schwarz, Nina, and Ameer M. Manceur. 2014. "Analyzing the Influence of Urban Forms on Surface Urban Heat Islands in Europe." *Journal of Urban Planning and Development* 141 (3): A4014003. doi:10.1061/(ASCE)UP.1943-5444.0000263.
- Seirup, L, and G Yetman. 2006. "U.S. Census Grids (Summary File 3), 2000." Palisades, NY: NASA Socioeconomic Data and Applications Center (SEDAC).
- Shapiro, S. S., and M. B. Wilk. 1965. "An Analysis of Variance Test for Normality (Complete Samples)." *Biometrika* 52 (3/4): 591–611.
- Skelhorn, Cynthia P., Geoff Levermore, and Sarah J. Lindley. 2016. "Impacts on Cooling Energy Consumption due to the UHI and Vegetation Changes in Manchester, UK." *Energy and Buildings* 122. Elsevier B.V.: 150–59. doi:10.1016/j.enbuild.2016.01.035.

- Smoliak, Brian V., Peter K. Snyder, Tracy E. Twine, Phillip M. Mykleby, and William F. Hertel. 2015. "Dense Network Observations of the Twin Cities Canopy-Layer Urban Heat Island." *Journal of Applied Meteorology and Climatology* 54 (9): 1899–1917. doi:10.1175/JAMC-D-14-0239.1.
- Stone, Brian, Jeremy J. Hess, and Howard Frumkin. 2010. "Urban Form and Extreme Heat Events: Are Sprawling Cities More Vulnerable to Climate Change than Compact Cities?" *Environmental Health Perspectives* 118 (10): 1425–28. doi:10.1289/ehp.0901879.
- Streutker, David R. 2003. "A Study of the Urban Heat Island of Houston, Texas." Rice University.
- Susca, T., S. R. Gaffin, and G. R. Dell'Oso. 2011. "Positive Effects of Vegetation: Urban Heat Island and Green Roofs." *Environmental Pollution* 159 (8-9): 2119–26. doi:10.1016/j.envpol.2011.03.007.
- Swan, Lukas G., and V. Ismet Ugursal. 2009. "Modeling of End-Use Energy Consumption in the Residential Sector: A Review of Modeling Techniques." *Renewable and Sustainable Energy Reviews* 13 (8): 1819–35. doi:10.1016/j.rser.2008.09.033.
- Team, R Core. 2017. "R: A Language and Environment for Statistical Computing." Vienna, Austria.
- Todhunter, Paul E. 1996. "Environmental Indices for the Twin Cities Metropolitan Area (Minnesota, USA) Urban Heat Island - 1989." *Climate Research* 6 (1): 59–69. doi:10.3354/cr006059.
- Tran, Hung, Daisuke Uchiyama, Shiro Ochi, and Yoshifumi Yasuoka. 2006. "Assessment with Satellite Data of the Urban Heat Island Effects in Asian Mega Cities." *International Journal of Applied Earth Observation and Geoinformation* 8 (1): 34–48. doi:10.1016/j.jag.2005.05.003.
- Tso, C. P. 1994. "The Impact of Urban Development on the Thermal Environment of Singapore." In *The Report of the Technical Conference on Tropical Urban Climates*. Dhaka: WMO.
- University, Center for International Earth Science Information Network - CIESIN - Columbia. 2017. "Gridded Population of the World, Version 4 (GPWv4): Population Count, Revision 10." Palisades, NY: NASA Socioeconomic Data and Applications Center (SEDAC). <https://doi.org/10.7927/H4PG1PPM>.
- Vahmani, P., and George A. Ban-Weiss. 2016. "Impact of Remotely Sensed Albedo and Vegetation Fraction on Simulation of Urban Climate in WRF-Urban Canopy Model: A Case Study of the Urban Heat Island in Los Angeles." *Journal of Geophysical Research: Atmospheres* 121: 1511–31. doi:10.1002/2015JD023718.

- Vallati, Andrea, Andrea De Lieto Vollaro, Iacopo Golasi, Eugenio Barchiesi, and Carlo Caranese. 2015. "On the Impact of Urban Micro Climate on the Energy Consumption of Buildings." *Energy Procedia* 82. Elsevier B.V.: 506–11. doi:10.1016/j.egypro.2015.11.862.
- Vardoulakis, E., D. Karamanis, A. Fotiadi, and G. Mihalakakou. 2013. "The Urban Heat Island Effect in a Small Mediterranean City of High Summer Temperatures and Cooling Energy Demands." *Solar Energy* 94 (August): 128–44. doi:10.1016/j.solener.2013.04.016.
- Verkade, J. S., J. D. Brown, F. Davids, P. Reggiani, and A. H. Weerts. 2017. "Estimating Predictive Hydrological Uncertainty by Dressing Deterministic and Ensemble Forecasts; a Comparison, with Application to Meuse and Rhine." *Journal of Hydrology* 555. The Author(s): 257–77. doi:10.1016/j.jhydrol.2017.10.024.
- Vose, R S, R L Schmoyer, P M Steurer, T C Peterson, R Heim, T Karl, and J Eischeid. 1992. "The Global Historical Climatology Network: Long-Term Monthly Temperature, Precipitation, Sea Level Pressure, and Station Pressure Data." *Journal Name: CDIAC Communications; Journal Issue: 17; Other Information: PBD: Sum 1992*, 309. doi:10.3334/CDIAC/cli.ndp041.
- Wackernagel, H. 1998. *Multivariate Geostatistics: An Introduction With Applications*. 2nd ed. Berlin: Springer.
- Watkins, R, J Palmer, M Kolokotroni, and P Littlefair. 2002. "The London Heat Island: Results from Summertime Monitoring." *Building Services Engineering Research and Technology* 23 (2002): 97–106. doi:10.1191/0143624402bt031oa.
- Xu, Hanqiu. 2010. "Analysis of Impervious Surface and Its Impact on Urban Heat Environment Using the Normalized Difference Impervious Surface Index (NDISI)." *Photogrammetric Engineering & Remote Sensing* 76 (5): 557–65. doi:10.14358/PERS.76.5.557.
- Xu, Hanqiu, Dongfeng Lin, and Fei Tang. 2013. "The Impact of Impervious Surface Development on Land Surface Temperature in a Subtropical City: Xiamen, China." *International Journal of Climatology* 33 (8): 1873–83. doi:10.1002/joc.3554.
- Yang, X C, Y L Zhang, L S Liu, W Zhang, M J Ding, and Z F Wang. 2009. "Sensitivity of Surface Air Temperature Change to Land Use/cover Types in China." *Science in China Series D-Earth Sciences* 52 (8): 1207–15. doi:10.1007/s11430-009-0085-0.
- Yang, Xuchao, Yiling Hou, and Baode Chen. 2011. "Observed Surface Warming Induced by Urbanization in East China." *Journal of Geophysical Research Atmospheres* 116 (14): 1–12. doi:10.1029/2010JD015452.
- Zhang, Hengyue, Menglin Jin, and Martin Leach. 2017. "A Study of the Oklahoma City Urban Heat Island Effect Using a WRF/Single-Layer Urban Canopy Model, a Joint

- Urban 2003 Field Campaign, and MODIS Satellite Observations.” *Climate* 5 (3): 72. doi:10.3390/cli5030072.
- Zhang, Kai, Evan M. Oswald, Daniel G. Brown, Shannon J. Brines, Carina J. Gronlund, Jalonne L. White-Newsome, Richard B. Rood, and Marie S. O’Neill. 2011. “Geostatistical Exploration of Spatial Variation of Summertime Temperatures in the Detroit Metropolitan Region.” *Environmental Research* 111 (8). Elsevier: 1046–53. doi:10.1016/j.envres.2011.08.012.
- Zhao, Hai-xiang, and Frédéric Magoulès. 2012. “A Review on the Prediction of Building Energy Consumption.” *Renewable and Sustainable Energy Reviews* 16 (6): 3586–92. doi:10.1016/j.rser.2012.02.049.
- Zhao, Lei, Xuhui Lee, Ronald B. Smith, and Keith Oleson. 2014. “Strong Contributions of Local Background Climate to Urban Heat Islands.” *Nature* 511 (7508). Nature Publishing Group: 216–19. doi:10.1038/nature13462.
- Zhou, Decheng, Shuqing Zhao, Shuguang Liu, and Liangxia Zhang. 2014. “Spatiotemporal Trends of Terrestrial Vegetation Activity along the Urban Development Intensity Gradient in China’s 32 Major Cities.” *Science of the Total Environment* 488–489 (1). Elsevier B.V.: 136–45. doi:10.1016/j.scitotenv.2014.04.080.
- Zhou, L., R. E. Dickinson, Y. Tian, J. Fang, Q. Li, R. K. Kaufmann, C. J. Tucker, and R. B. Myneni. 2004. “Evidence for a Significant Urbanization Effect on Climate in China.” *Proceedings of the National Academy of Sciences* 101 (26): 9540–44. doi:10.1073/pnas.0400357101.
- Zhou, Yuyu, Steven J Smith, Kaiguang Zhao, Marc Imhoff, Allison Thomson, Ben Bond-Lamberty, Ghassem R Asrar, Xuesong Zhang, Chunyang He, and Christopher D Elvidge. 2015. “A Global Map of Urban Extent from Nightlights.” *Environmental Research Letters* 10 (5). IOP Publishing: 054011. doi:10.1088/1748-9326/10/5/054011.
- Zhou, Yuyu, Steven J. Smith, Christopher D. Elvidge, Kaiguang Zhao, Allison Thomson, and Marc Imhoff. 2014. “A Cluster-Based Method to Map Urban Area from DMSP/OLS Nightlights.” *Remote Sensing of Environment* 147. Elsevier Inc.: 173–85. doi:10.1016/j.rse.2014.03.004.
- Zhou, Yuyu, Qihao Weng, Kevin R. Gurney, Yanmin Shuai, and Xuefei Hu. 2012. “Estimation of the Relationship between Remotely Sensed Anthropogenic Heat Discharge and Building Energy Use.” *ISPRS Journal of Photogrammetry and Remote Sensing* 67 (1). International Society for Photogrammetry and Remote Sensing, Inc. (ISPRS): 65–72. doi:10.1016/j.isprsjprs.2011.10.007.